SEISMIC SOURCE DISCRIMINATION IN THE WASATCH PLATEAU REGION OF CENTRAL UTAH

by

Jared Robert Stein

A thesis submitted to the faculty of
The University of Utah
in partial fulfillment of the requirements for the degree of

Master of Science

in

Geophysics

Department of Geology and Geophysics

The University of Utah

May 2016

The University of Utah Graduate School

STATEMENT OF THESIS APPROVAL

The thesis of **Jared Robert Stein**

has been approved by the following supervisory committee members:

Kristine Louise Pankow	, Chair	**11/02/2015** Date Approved
Keith David Koper	, Member	**11/02/2015** Date Approved
John M. Bartley	, Member	**11/02/2015** Date Approved

and by **John M. Bartley** , Chair of

the Department of **Geology and Geophysics**

and by David B. Kieda, Dean of The Graduate School.

ABSTRACT

The Wasatch Plateau region of Central Utah contains multiple sources of seismic activity caused by a complicated mix of extensional tectonics and a long history of coal mining induced seismicity (MIS). This combination of seismic source types has made it difficult to study this region effectively as conclusions about regional structure, seismic hazard, and mine planning rely on knowing the causes of the events within an earthquake catalog. Using a catalog of 6,402 events recorded at University of Utah Seismograph Stations broadband seismic station SRU between mid-1998 and the end of 2011, this study aims to identify seismic event types in this region through a combination of methods. After updating the event locations in the catalog using more detailed velocity models and a newer location algorithm, all events in the catalog are cross-correlated with each other to quantify the level of waveform similarity. Clusters of similar waveforms are determined with a single-link clustering algorithm in a computer program called *Detex*. The locations, depth distributions, first motions, and spectral content of these clusters are then compared to clusters of known source types to determine whether the events in each cluster are MIS, tectonic earthquakes, or ambiguous. From this analysis, I determine that this study area contains 5,227 events in 38 clusters that are MIS, 310 events in 46 clusters that are not a result of mining operations, and 865 events that have unknown source

types. The resulting catalog reveals the existence and extent of tectonic activity taking place within the mine boundaries in the Central Wasatch Plateau.

TABLE OF CONTENTS

LIST OF FIGURES

ACKNOWLEDGEMENTS

I would like to thank the National Institute for Occupational Safety and Health and the state of Utah for funding this research. I would also like to thank Jim Pechmann, Mark Hale, Katherine Whidden, Paul Roberson, Bill Blycker, and Relu Burlacu for all of their knowledge and insight; my fellow graduate students for being such wonderful colleagues and friends; Derrick Chambers for technical support and the use of his *Detex* program; John Bartley and Keith Koper for serving on my committee; and Kris Pankow for serving as my advisor and providing an immeasurable amount of help and guidance along the way.

CHAPTER 1

INTRODUCTION

Due to a unique set of geologic and man-made conditions, the state of Utah is home to many different types of seismic events including those caused by extensional tectonic forces and those caused by human activity [*Arabasz et al.,* 2007, *Stump et al.*, 2007]. In order to better understand the different types of seismic activity, one must first classify the seismic events based on category. In this study, I examine several methods to create a catalog of seismic events located in the Wasatch Plateau region of central Utah discriminated by seismic source.

1.1 Geologic and Seismotectonic Setting

The Intermountain Seismic Belt (ISB) is a continuous band of seismicity that runs from Montana to Arizona [*Smith and Arabasz,* 1991]. In the Wasatch Plateau region of central Utah, the ISB follows the transition zone separating the actively deforming Basin and Range and the relatively stable Colorado Plateau physiographic provinces (Figure 1.1). This line of seismicity roughly follows the Interstate-15 corridor through the state of Utah and poses a substantial seismic hazard to the major population centers due to a history of magnitude 5+ earthquakes taking place along this transition zone [*Arabasz et*

al., 2007].

Seismic hazard throughout much of the state is difficult to quantify because of the long recurrence interval of significant earthquakes, the relatively sparse spacing of seismic stations in the central portion of the state, and the wide scatter of smaller events [*Arabasz et al.*, 2007]. Hazard in this area is further complicated by the presence of mining-induced seismicity (MIS) interspersed with these smaller earthquakes.

1.2 Mining-induced Seismicity

A number of underground coal mines have been in operation in central Utah since the late 1800s. Many of these operations are still active or have been active very recently (Figure 1.2). These mines use various methods of retreat mining where the roof of the mine is designed to collapse behind the active mining, resulting in a continuous series of ground motions following the progress of coal extraction. This activity has resulted in a well-known history of MIS [*e.g., Wong,* 1985; *Arabasz* et al., 1997; *Arabasz and Pechmann*, 2001].

The majority of MIS is observed as a relatively continuous sequence of small events that follow the mining process both spatially and temporally and are located at or very close to the depth of the mining activity [*Boltz et al.,* 2014]. However, violent failures of the roof or rockbursts (failure of the supporting pillars due to high vertical stress) can take place resulting in a significant danger to those working nearby [e.g., *Gale et al.*, 2001, *Iannacchione et al.,* 2005]. These failures can result in high magnitude seismic events like the M_L 3.9 Crandall Canyon Mine collapse that took place in 2007 [*Ford et al.,* 2008; *Pechmann et al.,* 2008; *Kubacki et al.,* 2014], and two similarly sized

events (M_L 3.8 and M_L 4.2) at Willow Creek Mine in 1998 and 2000 [*Arabasz and Pechmann*, 2001]. A better understanding of the relationship between mining activity and the pattern of observed seismicity could give mine operators valuable information in preventing or mitigating future incidents.

The nearly continuous seismic activity unrelated to tectonic processes taking place in central Utah has made it difficult to study the natural seismicity of the region and to assess the seismic hazard in the region. Discrimination of MIS from naturally occurring earthquakes allows for more accurate studies of the regional structure and tectonic setting. It also allows for better characterization of MIS and how it might relate to ground control issues.

There has been recent interest in characterizing the seismic hazard posed by induced earthquakes, particularly in the oil and gas fields of the central United States, and incorporating these continuously changing source types into the National Seismic Hazard Maps [*Petersen et al.,* 2015]. Typically, MIS events are not taken into account in the production of seismic hazard maps, but efforts to incorporate these events are under development [*Petersen et al,* 2014] and will require separate catalogs of MIS and tectonic events.

1.3 Methodology of Study

While the task of discriminating between event types might appear straightforward, limitations in seismic network coverage in the Wasatch Plateau have made constraining the depth of seismic events (the first-order discriminant) in that region difficult. The discrimination of MIS from tectonic seismicity in the Wasatch Plateau has

been an ongoing area of investigation. *Arabasz and Pechmann* [2001] attribute the majority of seismic events in this area to mining activity based on the spatial correlation between seismic event epicenters and the distribution of mine permit areas, as well as correlations between seismicity and production rates. *Pechmann et al.* [2008] use the distinct waveform characteristics of mine collapses (emergent waveforms and low frequency energy) compared to typical earthquakes (impulsive P-arrivals and clear S-energy) to discriminate event types. *Ford et al.* [2008] inverted the waveforms to determine full moment tensors and evaluated the source type based on the percent of double-couple contribution.

In this study, using the University of Utah Seismograph Stations (UUSS) seismicity catalog filtered for events located in the Wasatch Plateau (Figure 1.3), I apply four analysis tools to discriminate MIS from tectonic earthquakes. The first tool, *HYPOINVERSE-2000* [*Klein*, 2001], was used to generate higher precision locations than previously determined. Using these new locations, events are discriminated by depth. The second tool, *Detex* [*Chambers et al.,* 2015], uses waveform cross-correlation applied to a subset of events recorded between mid-1998 and the end of 2011 to cluster events based on waveform similarity. Waveforms from events with similar mechanisms and locations have high correlation values, while waveforms from events spatially separated or with differing mechanisms are poorly correlated. Based on the assumption that each cluster created by *Detex* is a list of events with the same source type, each cluster is discriminated as a whole rather than each individual event in the catalog. The third tool used was P-wave spectral analysis of each event. This method is based on the observation that MIS events and tectonic earthquake events have different frequency content in the

first few seconds of signal. Lastly, the first motions of each event as determined by UUSS analysts at the time of the event's initial location were examined to search for events with mixed first motions suggestive of tectonic earthquakes and events with all observed first motions as dilatational suggestive of a predominantly implosional source characteristic of mine collapses [*Wong et al.,* 1989]. Using all of these tools together, the aim of this study is to identify the subset of seismic events that are the result of mining and exclude them from the catalog of seismicity in the Wasatch Plateau.

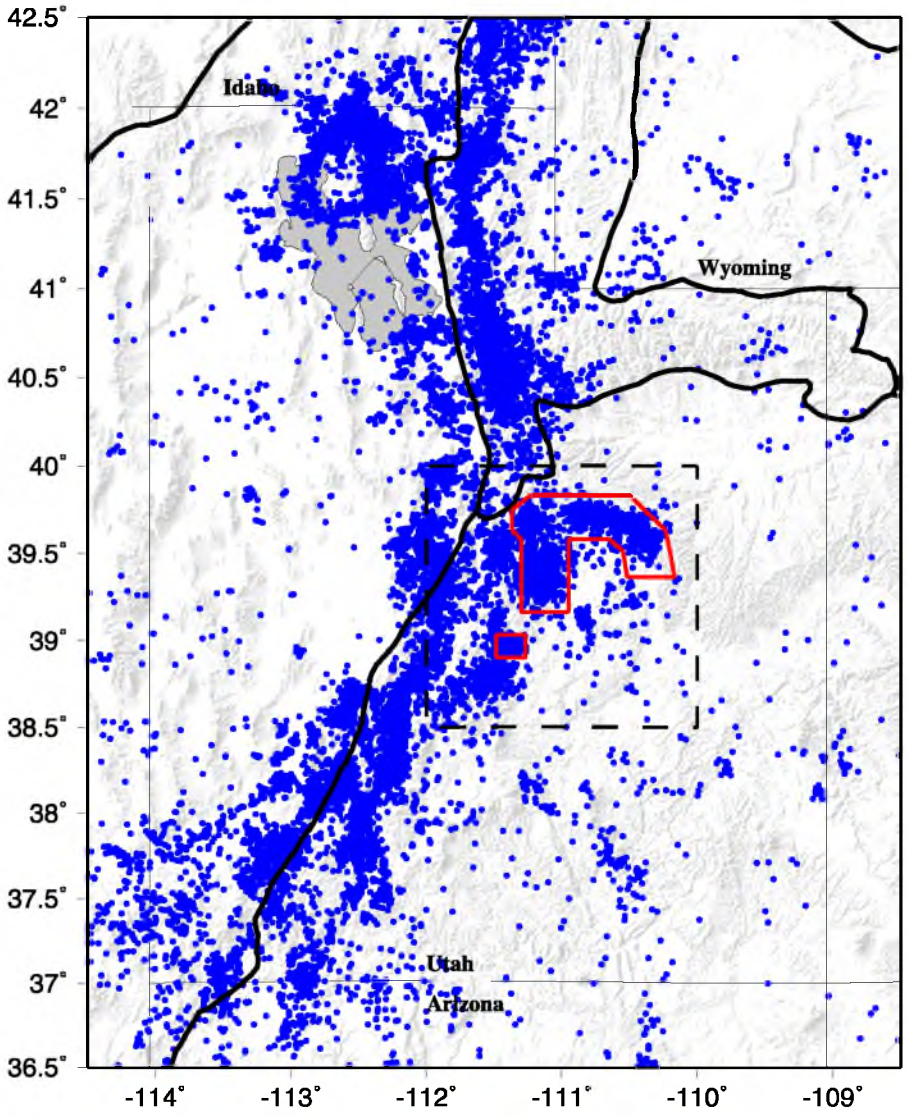

Figure 1.1. Map of seismicity in Utah. Blue dots (N = 88,768) are seismic events detected by UUSS in and around the state of Utah between 1981 and 2012. The solid black lines indicate the boundaries of the Central Rocky Mountains in the north, the Basin and Range to the west, and the Colorado Plateau to the east. Red polygons represent the underground coal mining region of Utah. The black dashed line box is shown in greater detail in Figure 1.2.

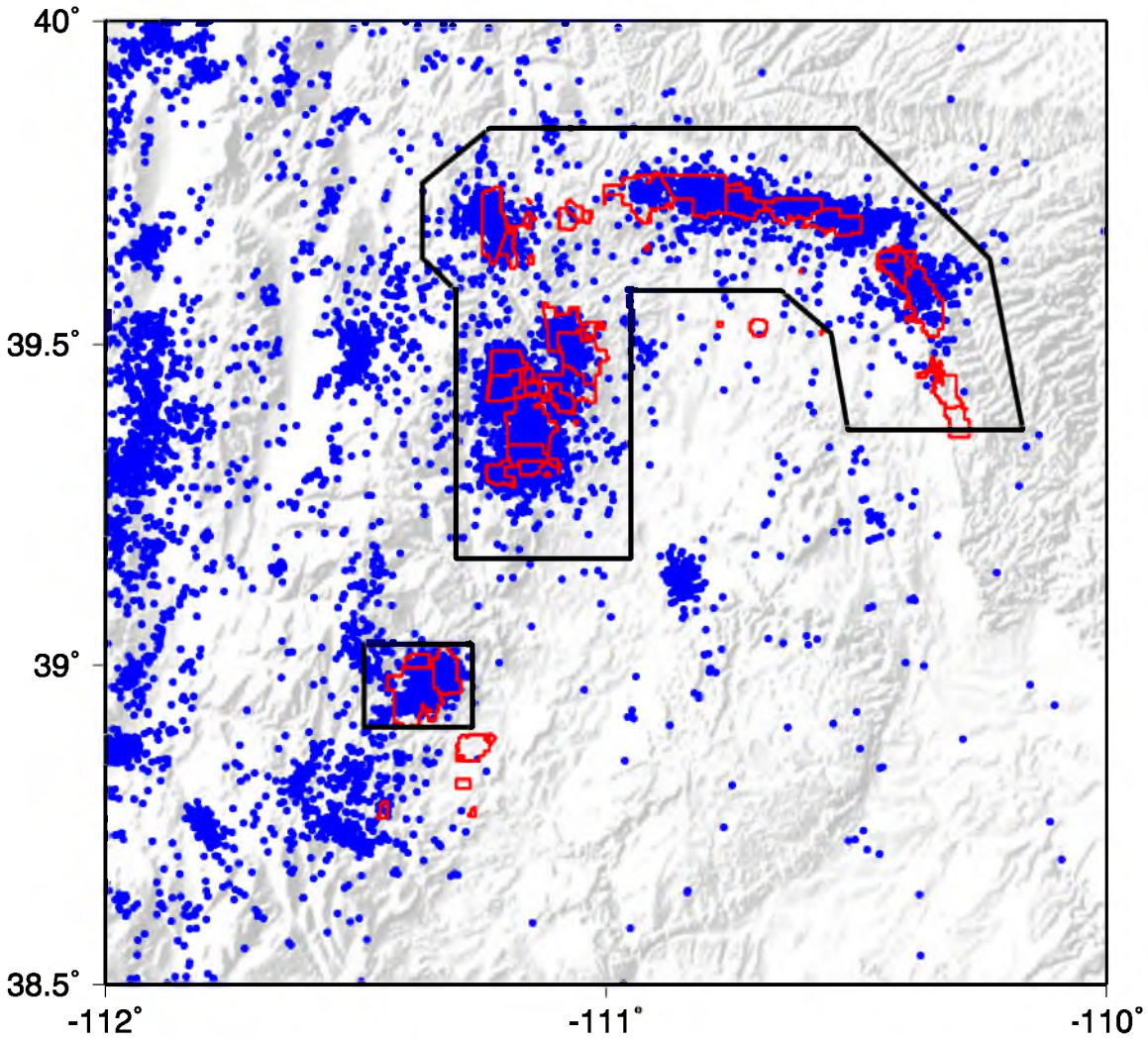

Figure 1.2. Map of mining region. The general extent of coal mining in Utah is indicated with the black polygons while individual mine permit boundaries are shown in red. Blue dots (N = 26,009) are seismic events detected by UUSS between 1981 and 2012.

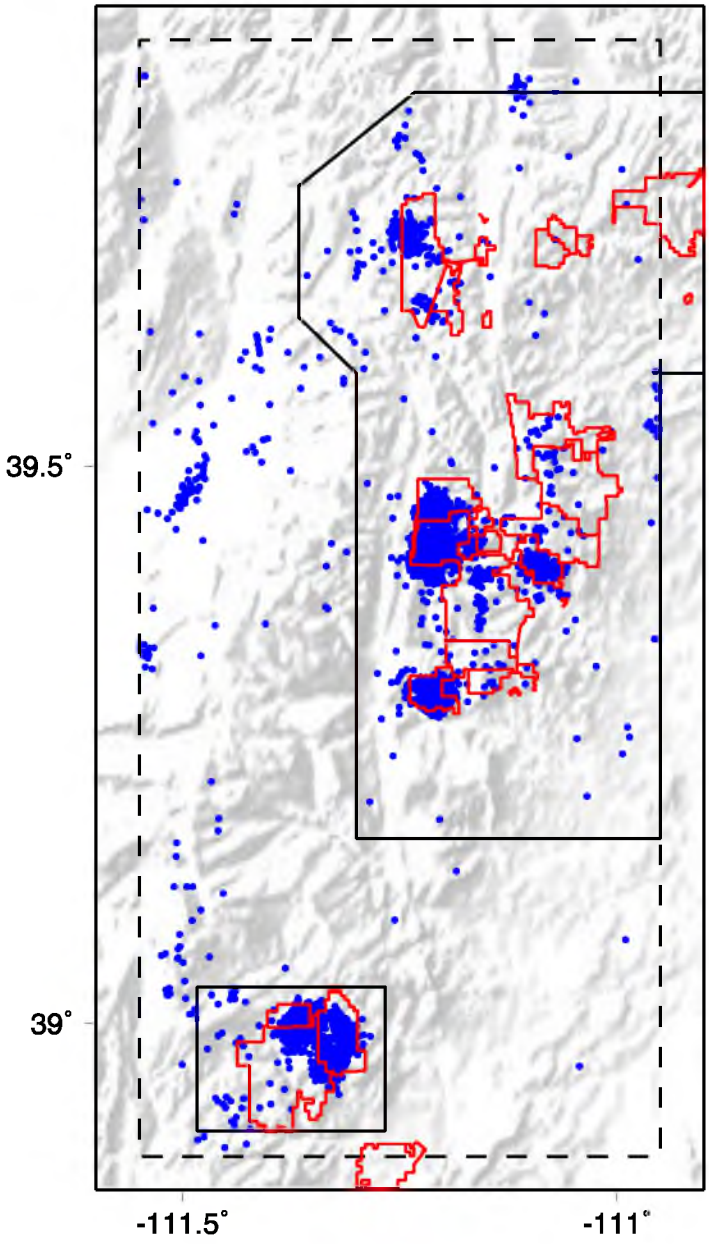

Figure 1.3. Map of study area. The dashed box defines the study area and contains 7,544 seismic events (blue dots) with analyst-determined P-arrival time picks at UUSS station SRU between September 1998 to December 2011. Individual mine permit boundaries are red polygons, and the boundary of the mining region is shown with the solid black line.

CHAPTER 2

RELOCATION OF EVENT CATALOG

The first (and possibly most obvious) method to discriminate MIS from natural tectonic earthquakes is to simply categorize events as MIS if they occurred at mine level (within 2 km of the Earth's surface) and within known mine boundaries, and those occurring much deeper and/or outside the permit boundaries as tectonic earthquakes. Unfortunately, the depth of seismic events in this region is difficult to constrain due to limitations in network coverage and the shallow nature of mining seismicity. In general, the depth of any seismic event can be considered well constrained if the distance between the epicenter and the nearest station is no more than the focal depth or 1.4 times the focal depth if there is an accurate S-pick [*Gomberg et al.*, 1990]. Figure 2.1 shows all of the stations installed in the state of Utah used for locating events within the study area, including those in temporary arrays. Although UUSS has deployed a relatively dense station geometry, coal is rarely mined deeper than a few kilometers. As a result, it is unusual to have an event occur close enough to a seismic station to accurately constrain the depth, and deploying new stations at the necessary density would be extremely costly.

2.1 Catalog Relocations

Before October 1, 2012, event locations reported by UUSS were determined using P- and S-arrival times at stations within the UUSS network and processed with *HYPOINVERSE* [*Klein*, 1978], which was configured to use three velocity models: Basin and Range, Colorado Plateau, and Yellowstone, depending on station location [*Burlacu et al.,* 2013]. On October 1, 2012, the location process was updated to a newer version of *HYPOINVERSE* called *HYPOINVERSE-2000* [*Klein*, 2001], and several improvements to the location procedure were made. Additional velocity models, including one specifically for the mining region [*Arabasz et al.*, 2002] were added, and the velocity model was determined by the location of the seismic event allowing for more specific conditions to be accounted for. Additionally, the top of the velocity model, or datum, was raised from 1.5 km above sea level for the Wasatch Plateau Region, to 3.5 km above sea level for the entire network to allow for much shallower events to be located without using ad hoc elevation corrections, and use actual station elevations to properly calculate travel times. In the mining region, some stations are located below mine level increasing the 3-D distribution of the network. All events are now reported relative to sea level.

Since I am primarily concerned with seismic events from before this update was made, the first step of this study was to update the pre-2012 locations using the new software and velocity models. This provides more accurate locations than the original catalog and standardizes the process across all years of data.

It is important to remember that, although the catalog can be updated with more accurate velocity models and station locations, the older the event, the fewer stations were installed in the network when it took place. As time goes on, more and more

stations have been installed in the UUSS network to fill gaps in coverage and to help to resolve the issues of location resolution mentioned above. Consequently, for times closer to the present, more events are recorded at smaller magnitudes, and these events typically have more accurate locations when compared to older events in the same region.

All 86,709 events from 1981 (when digital recording began) to the end of September of 2012 (when the current location algorithm was implemented) in the UUSS catalog were relocated with the new procedure to create an updated catalog for use in the remainder of this study. Figure 2.2 shows event locations before and after relocation, with depths binned into three groups. Most events moved only a small horizontal distance from their initial epicentral location as can be seen in Figure 2.3. However, after relocation, there is a notable shift in the depths of the events. There are now a number of events located at depths shallower than the previous datum, and the depths separate into three groups (Figure 2.4). The average depth for events in the study area moved from 2.70 km to 2.32 km below sea level. Additionally, there is a noticeable spike of relocated events at a depth of 6 km that is likely an artifact of the relocation process, as this is the starting depth at the beginning of the inversion.

2.2 First Motions

In addition to phase picks for each event, the UUSS catalog also contains first motions for many events. The first motion of a seismogram is simply the direction that the initial energy reaching the seismometer moved the ground. This is a simple observation but, when used in context of all of the stations recording signal from a particular event, information about the direction of slip of the fault can be determined.

Unfortunately, clear first motions are often difficult to observe due to interference with noise at the station, but for many events, several of the stations used for location will include a first motion along with their pick times.

First motions are useful when discriminating tectonic earthquakes from those caused by sources other than slip on a plane. For example, a typical tectonic earthquake should contain first motions of both compression (up) and dilatation (down) at different stations depending on where the station is located relative to the plane of slip and the auxiliary plane. Conversely, explosion and implosion sources have first motions in only one direction (up or down, respectively [*Stein and Wysession,* 2003]). In the context of discriminating MIS from tectonic earthquakes, this distinction is very important because tectonic earthquakes should have mixed first motions whereas MIS should yield only dilatational first motions because this source type is mostly implosional.

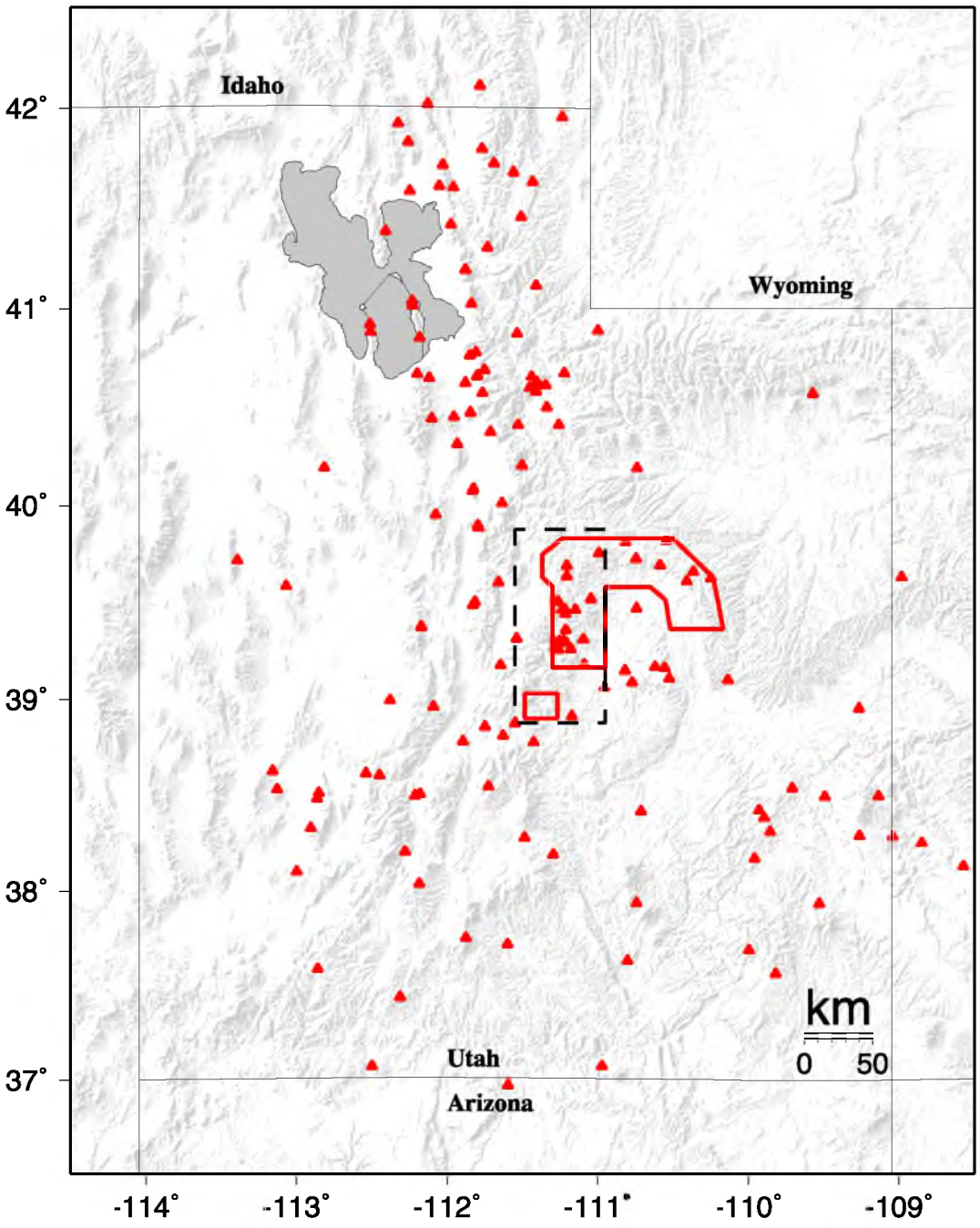

Figure 2.1. Map of UUSS network. Red triangles represent all stations used in relocation with *HYPOINVERSE-2000*. This includes many temporary stations that were only installed for a short time. Dashed rectangle denotes specific study area and red polygons show mining area.

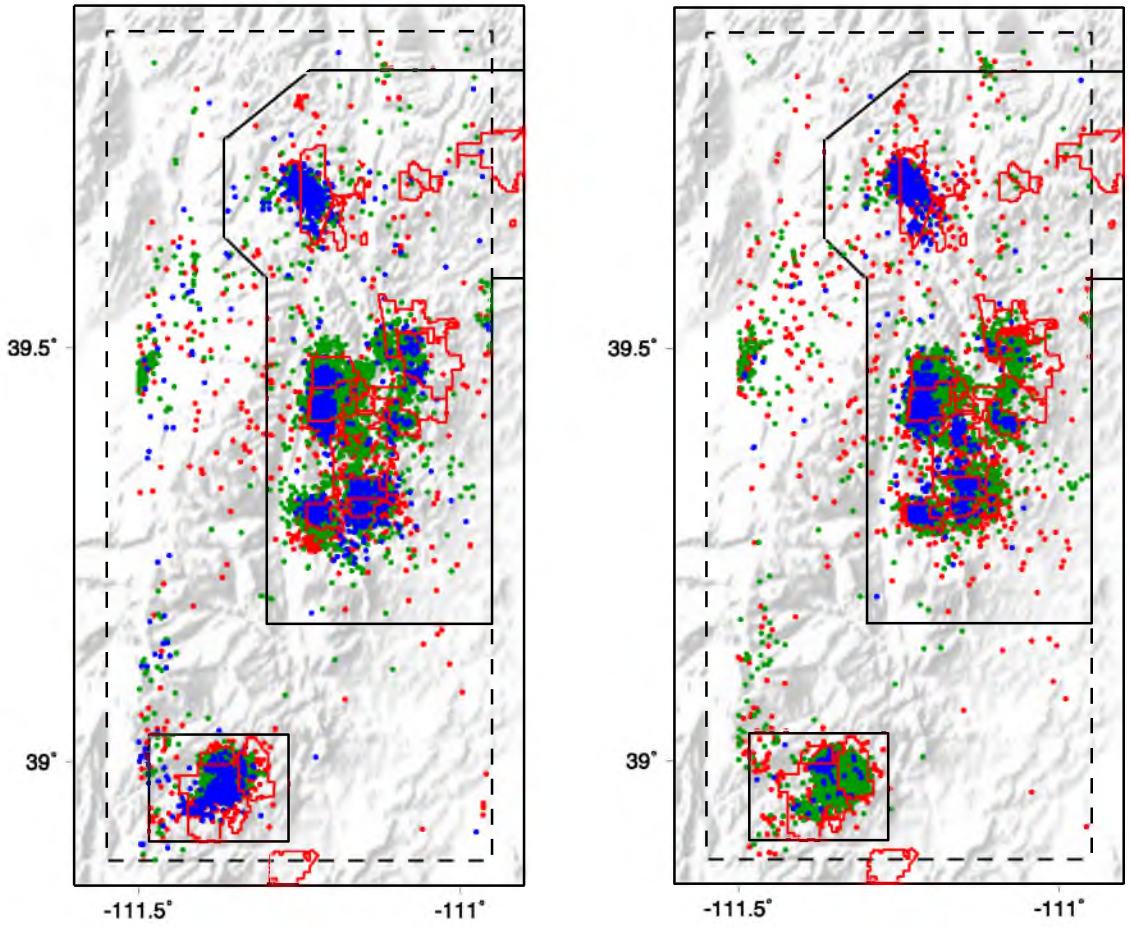

Figure 2.2. Seismicity before (left) and after (right) *HYPOINVERSE-2000* relocation. For both sets, events located above sea level are in blue, from 0 to 5 km are in green, and events deeper than 5 km are in red.

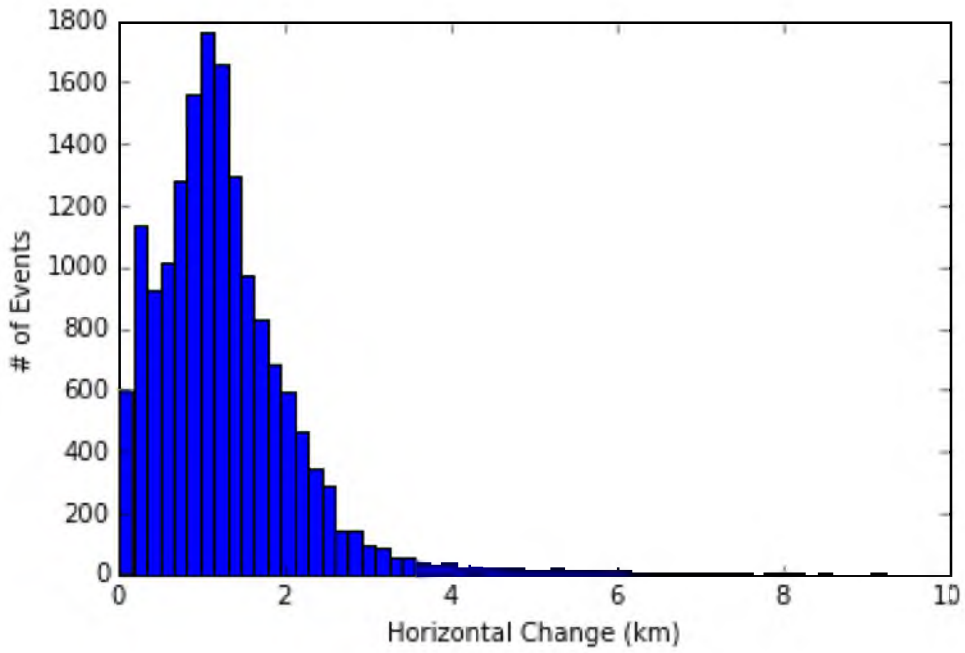

Figure 2.3. Horizontal (epicentral) change. Histogram of epicentral changes from initial catalog location to the new location with *HYPOINVERSE-2000*.

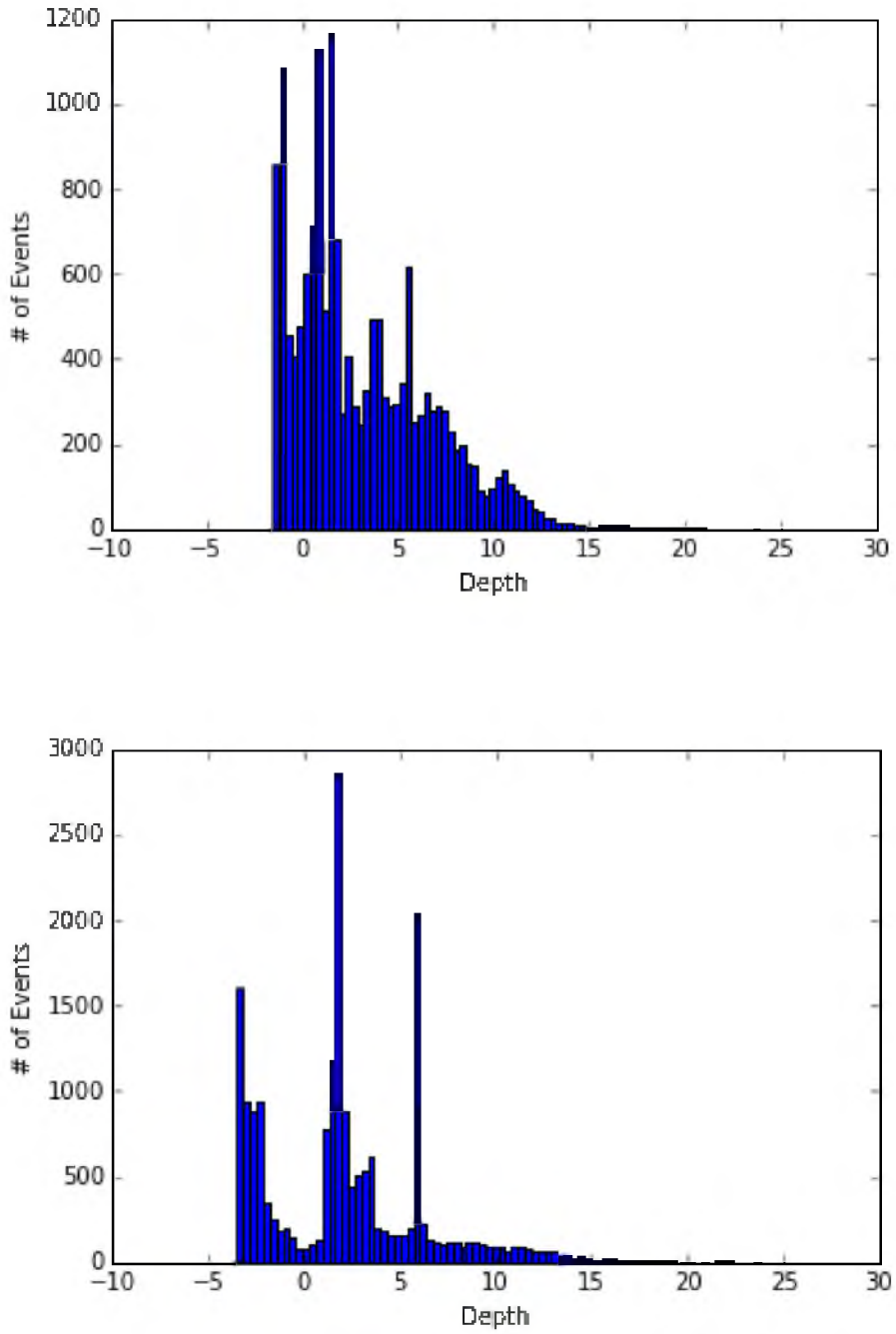

Figure 2.4. Depth distribution. Histograms of event depths before (top) and after (bottom) relocation (N = 16,576). Depths are relative to sea level.

CHAPTER 3

EVENT CLUSTERING USING WAVEFORM CROSS-CORRELATION

An increasingly popular technique in seismic processing is the use of cross-correlation to determine waveform similarity. This process uses a segment of seismic data recorded during a known event and scans it across a second seismogram to measure the similarity between the waveforms. This technique is often used to compare known seismic events with continuous data to search for previously undetected events in regions of natural or induced seismicity [e.g., *Schaff and Waldhauser,* 2010*; Kubacki et al.,* 2014], or for detecting explosions as part of nuclear monitoring programs [*Zhang and Wen,* 2015]. For the purpose of this study, instead of searching for new or previously undetected events, waveform cross-correlation is used to determine the degree of similarity among all individual seismic events detected in the study area with arrival time picks at station SRU between mid-1998 and the end of 2011.

When a seismic event is recorded, the seismic waves arriving at the station are the convolution of the instrument response, the source, and the medium in which the seismic waves travel between the source and receiver. Consequently, seismic events with similar sources and locations have similar waveforms and, the more these factors diverge, the more dissimilar their respective waveforms are. Earthquakes with greater depths and

different mechanisms do not correlate highly with shallow MIS (Figure 3.1). By forming clusters of similar events, I effectively reduce a catalog of individual events to a much shorter list of representative clusters to be more closely examined. The waveform similarity between events in a single cluster can be seen in Figure 3.2. For this study, these clusters are the basis for additional discrimination methods because I can assume events within a cluster are similar enough to each other that they are of the same source type.

3.1 Single Link Clustering

I use the *python*-based program *Detex* [*Chambers et al.*, 2015] to run a single-link clustering (sometimes referred to as hierarchical clustering) analysis of the waveforms for each event recorded at the UUSS three-component, broadband seismometer SRU, which is located approximately 40 km to the east of the study area (Figure 3.3). This station was selected because it is located near the study area and roughly equidistant from its northern and southern ends. SRU was installed in mid-1998; thus, the dataset analyzed includes events recorded from mid-1998 through the end of 2011, a total of 7,544 events. Waveform data for only 6,394 events could be retrieved from Incorporated Research Institutions of Seismology (IRIS) for analysis due to gaps in the data on any channel.

The single-link clustering algorithm of *Detex* follows the procedure outlined in *Harris* [2006]. Each event waveform is correlated with every other event waveform and a correlation coefficient between 0 and 1 is calculated. The correlation coefficients are then arranged to find the "nearest neighbor" of each event creating groups based on a predetermined threshold (0.7 for this study). If the event correlates more closely than this

value to any event in a cluster, it is then added to that cluster and, if any two events in two separate clusters correlate more closely than 0.7, the two clusters are joined together. It is important to note that using a correlation coefficient of 0.7 does not indicate that every event in a cluster is at least 70% similar to every other event in the cluster, but rather that every event in a cluster is at least 70% similar to at least one other event in the cluster. The result of this process can be visualized in an event dendrogram (Figure 3.4). This visualization can be particularly helpful in examining subclusters of very highly correlated events or examining how dissimilar any two events are from each other.

Mining operations cause continuously migrating seismicity that tracks progress along a mine plan of longwall panels or advancing and retreating sections. *Stein et al.* [2015] were able to describe the spatial and temporal progression of a single longwall coal mine in southern Utah over a ten year period. Single-link clustering of these events lends itself to the progression of the mining process—even though a panel might be several kilometers long, events at the beginning of the panel are linked to events located at the end of the panel (even though the waveforms have changed owing to the differences in location) through the single-link clustering.

3.2 Preprocessing of Event Waveforms

For each event in this study, waveform data were detrended, filtered between 1 Hz and 10 Hz using a bandpass Butterworth filter, and cut to 30 sec windows beginning 3 sec before the analyst P-arrival time pick. Since there is a large variability in distance between the events closest to the station and those farthest away (~40 km to ~80 km respectively), the window length was carefully chosen to be long enough to include both

P- and S- energy for the farthest events. For distances between the study area and station SRU, this window length includes the P- and S-phases, as well as regional surface waves. A window length of $3*(t_S-t_P)$ was used by *Arrowsmith and Eisner* [2006] and $2.8*(t_S-t_P)$ was used by *Baisch et al.* [2008] for similar studies. However, these studies considered much smaller areas of interest, and so such precision was not possible over the much larger area of the Wasatch Plateau. A 30 sec window was ultimately determined by considering the previous studies and by inspecting event waveforms from events located at the farthest distance from SRU to assure that enough of the signal was represented in the cross-correlation.

3.3 Determining the Correlation Coefficient

A correlation coefficient of 0.7 was chosen for this study, but this value varies between any two independent clustering analyses. Many factors can affect how closely events cluster such as window length, number of total events, frequency band, and signal to noise ratio, so a different value must be determined for any particular analysis. The goal is to maximize the tradeoff between highly correlated, tightly spaced clusters and clusters that more widely define a source type or region.

The value of 0.7 was used for this study after carefully examining the resulting dendrogram (Figure 3.4) and finding that this value is sufficiently conservative to identify many of the more tightly grouped clusters. Lowering this value would result in fewer clusters, as some of these smaller groups would combine into larger clusters. Using 0.7 resulted in 6,132 of the 6,402 events clustering into 165 clusters with 270 remaining isolated.

A map of the clustered events is included as Figure 3.5. Major clusters can be seen tightly spaced in the mining permit areas. Additionally, different clusters can be seen within each mine. This is particularly evident in the southern region of the study area where a single isolated mine contains several different clusters. This is consistent with the longwall extraction process used at this mine as many large, adjacent sections of coal are removed in sequence before the machinery is moved to start the process over again in a different area of the mine [*Stein et al.*, 2015].

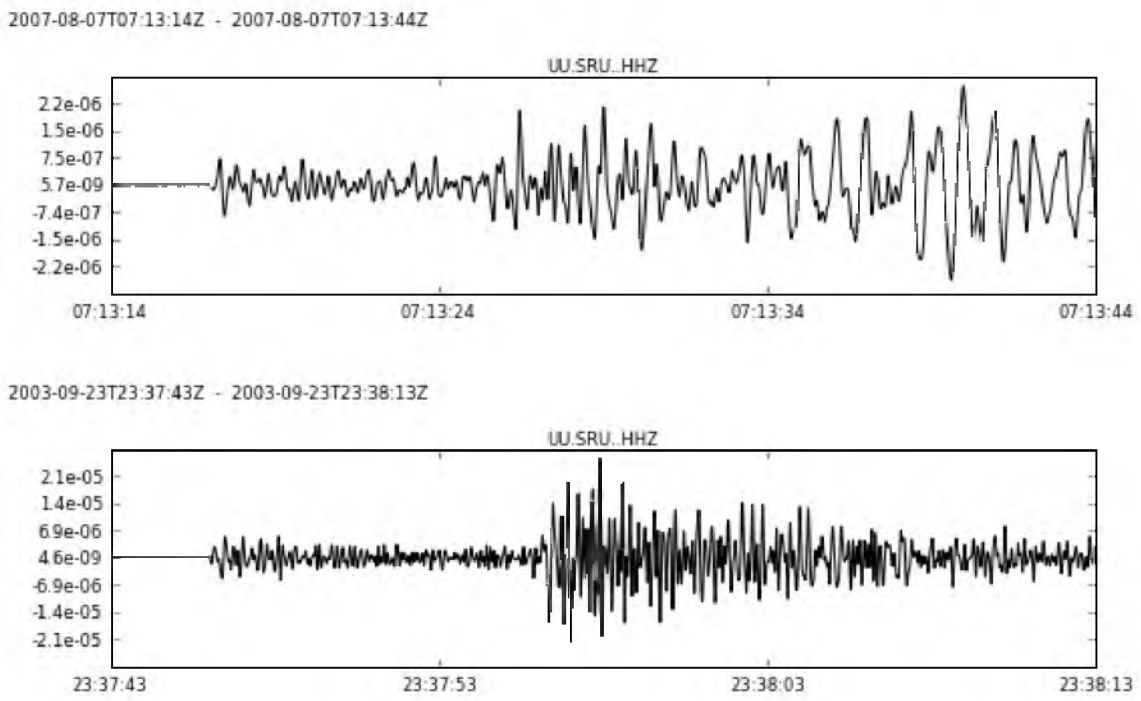

Figure 3.1. Difference between MIS and earthquake waveforms. The top figure is a known mining event and the bottom is a known earthquake. Both waveforms are from the vertical component of SRU filtered between 1 Hz and 10 Hz and cut to 30 sec starting 3 sec before the P-arrival time, the same magnitude of 2.4 (M_L), with distances to station of ~85 km and ~75 km, and depths of -2.91 km and 7.87 km respectively.

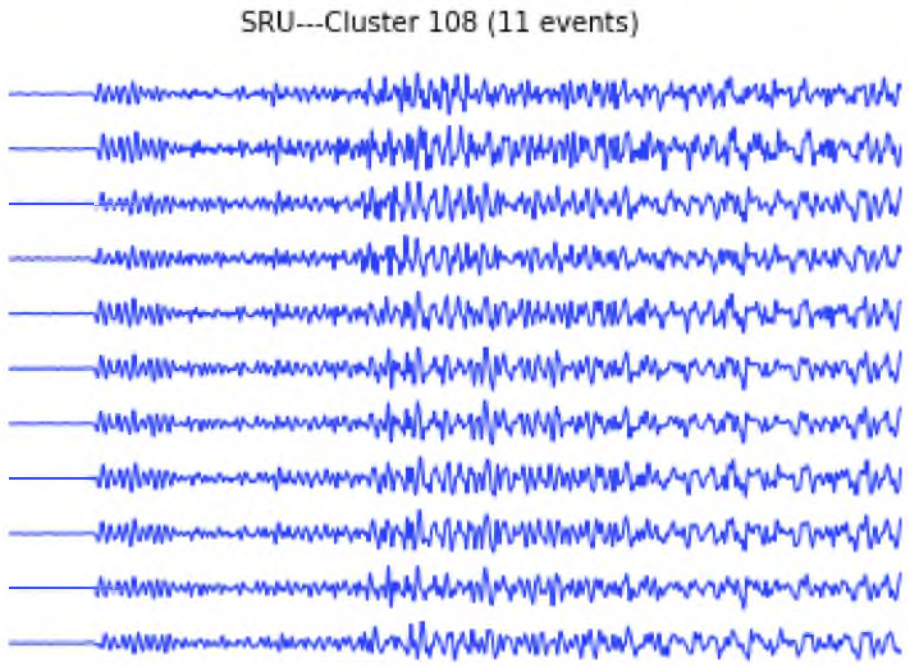

Figure 3.2. Waveform similarities. Individual waveforms that make up Cluster 108. Normalized waveforms are shown after preprocessing 30 sec window and bandpass filtering between 1 Hz and 10 Hz. Visual inspection of the waveforms confirms the similarity of events within the cluster.

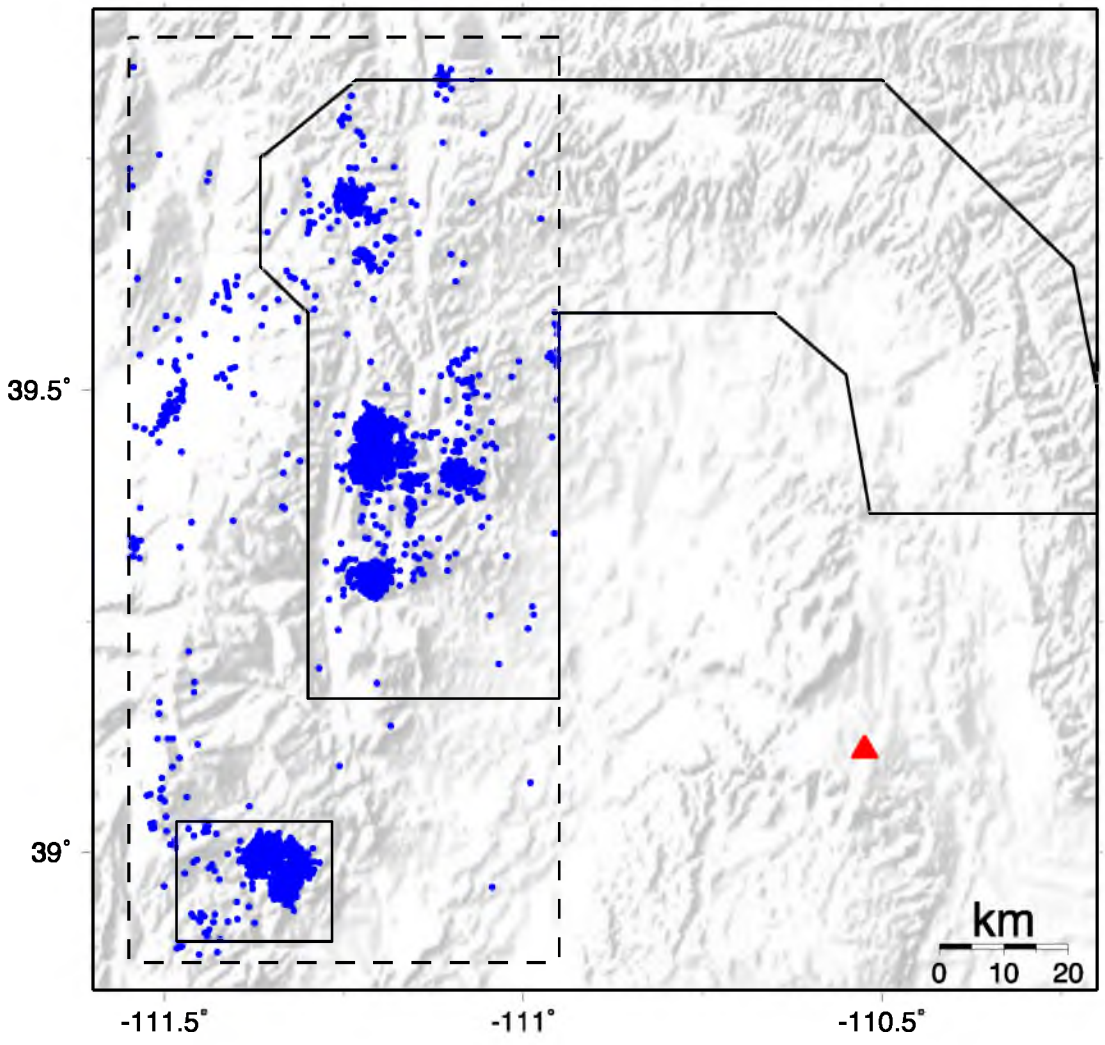

Figure 3.3. Location of UUSS seismic station SRU (red triangle) in relation to the study area (dashed box). Solid black polygons are the outlines of the mining region and blue dots are the events included in the clustering analysis N = 6,402.

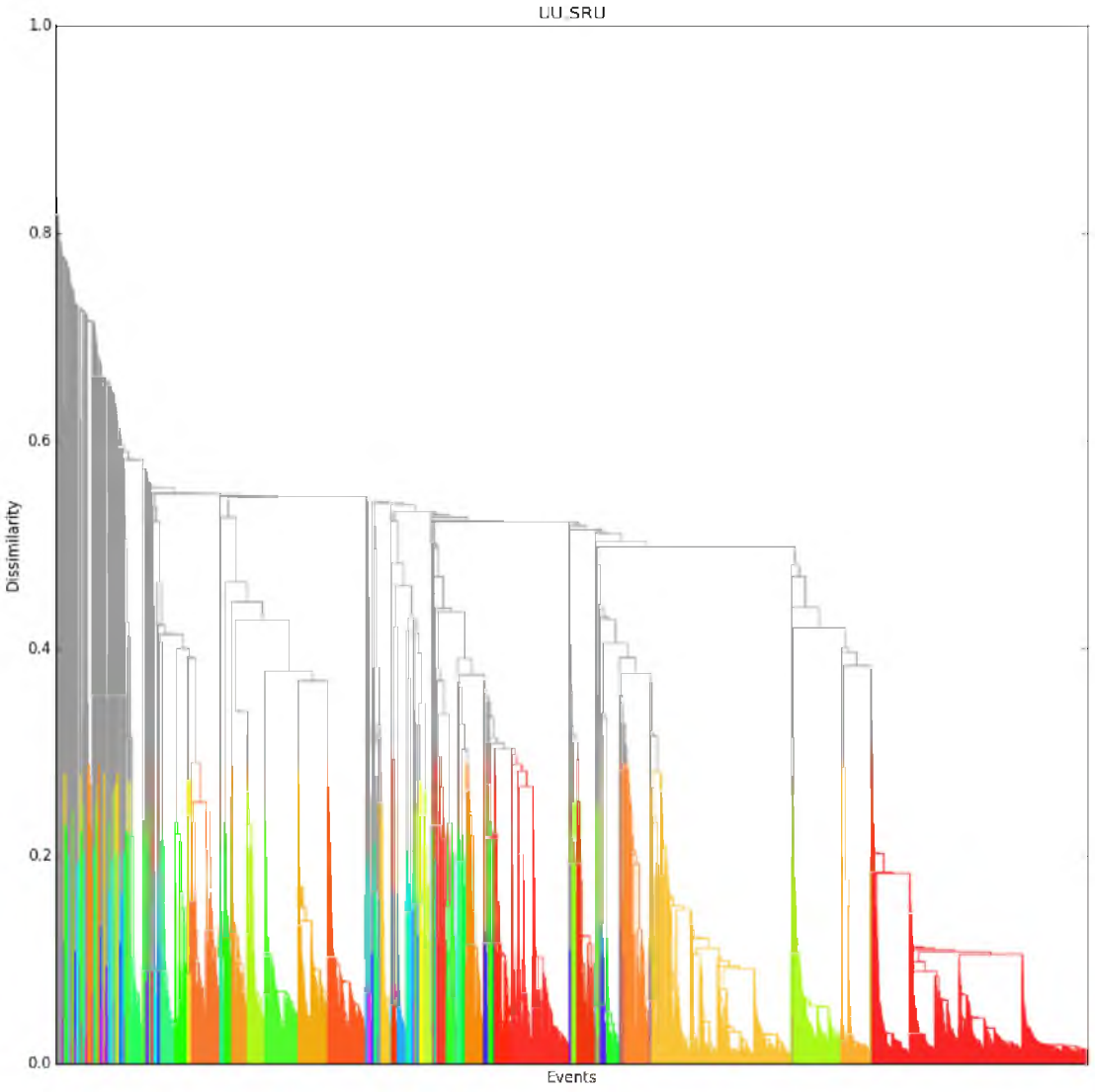

Figure 3.4. Dendrogram of all 6,394 events. Each vertical line represents an individual event, and each horizontal line indicates at what dissimilarity it correlates to its nearest neighbor. Each color represents a different cluster. Note that the y-axis is dissimilarity, which is equal to one minus the correlation coefficient.

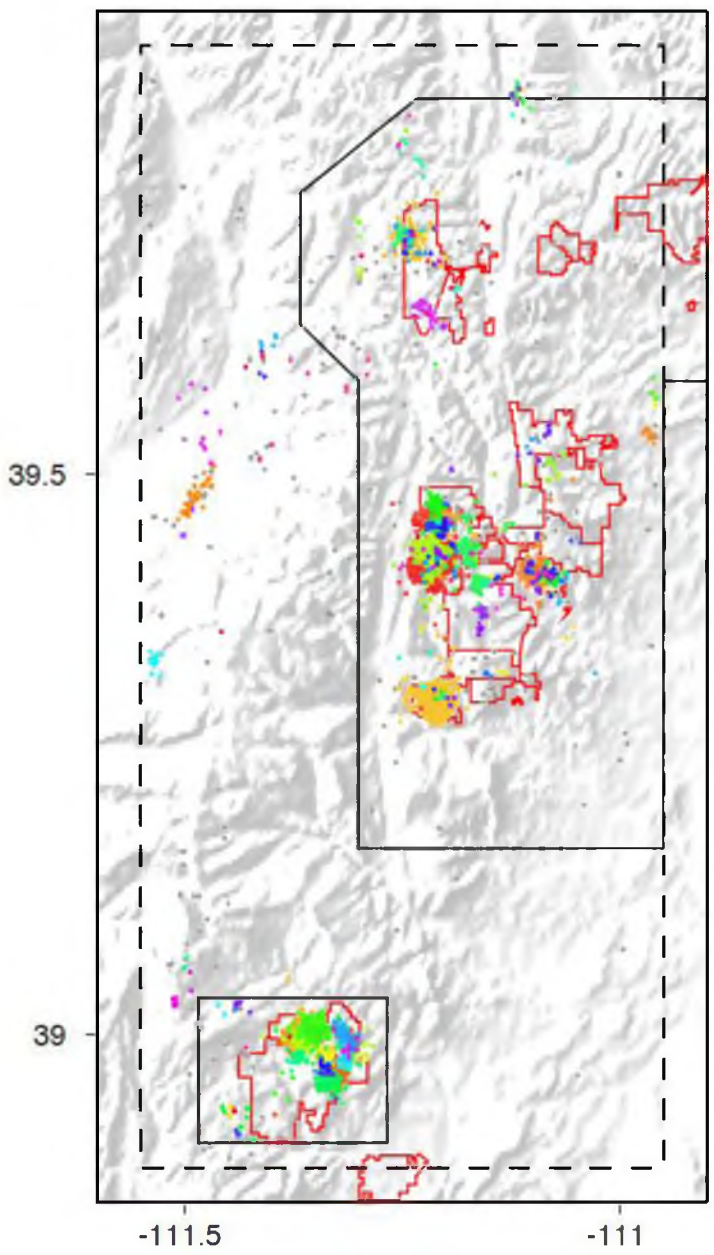

Figure 3.5. Cluster map. Events are shown in colors corresponding to the colors of the dendrogram of the previous figure. Note that events belonging to no cluster are shown in grey. Dashed line outlines the study area, individual mine permit boundaries are red polygons, and the boundary of the mining region is shown with the solid black line.

CHAPTER 4

SPECTRAL ANALYSIS

Figure 4.1 illustrates the difference in waveforms between a known mining event and a known tectonic earthquake. Each event has a magnitude of 2.4 and occurred at approximately the same distance from SRU. Despite these similarities, the two waveforms appear very different. When compared to the earthquake (bottom), the mining event (top) has a lower dominant frequency, a less distinct S-wave arrival, and larger surface waves. *Pechmann et al.* [2008] made these same observations when comparing the Crandall Canyon Mine collapse to a regional tectonic earthquake. These fundamental differences in waveform characteristics are the reason that cross-correlation can be used to sort events, but P-wave frequency content alone can be further examined to help discriminate event types.

4.1 Selecting Training Events for Spectral Analysis

In order to verify patterns in the frequency domain that indicate whether an event is MIS or a tectonic earthquake, a list of ground truth events is required. Twenty-six clusters from the single link clustering analysis in the previous chapter were identified as MIS by their location within the mine permit boundaries, shallow average depth, and

large cluster size. Additionally, 20 clusters and 62 isolated events were identified as tectonic earthquakes, as they were located within the study area but well outside of the mining boundaries. These two groups of events serve as the ground truth for the following frequency analysis.

4.2 Determining a Discriminant in the Frequency Domain

One of the most noticeable differences between MIS and tectonic earthquakes is the emergent signal that is recorded at the initial onset of an MIS event in contrast to the more impulsive first motions seen in typical tectonic earthquakes (Figure 4.1). This may be attributed to a difference in the way that stress is released in the two types of events. Typical mining events reflect piecewise collapse of undermined rock, whereas tectonic earthquakes result from release of elastic strain by fault slip, which for the small magnitude events considered in this study, is virtually instantaneous. The waveforms also may differ owing to the generally greater depth of tectonic events.

To more closely examine the initial energy differences in the onset of the two event types, each waveform from the ground truth catalog was cut from 0.5 sec before to 4.5 sec after the first arrival. *Allmann et al,* [2008] used a shorter window of 1.28 sec in a similar study that examined the initial energy of earthquakes and quarry blasts. However, in this study, a slightly longer window length was found to increase the differences in dominant frequency between the two event types.

Seismic traces from these groups were processed using the *python* package, *obspy* [*Beyreuther et al.,* 2010]. It is to be expected that events of different sizes have somewhat different spectral content, so events were binned by magnitude in increments of 0.5. For

each 5-sec waveform, a Nuttall taper was applied, and a fast Fourier transform was performed. With each waveform now in the frequency domain, each trace from each type of event was normalized. The normalized traces were then stacked together and averaged to create a representative spectral plot for both MIS and tectonic earthquakes in this catalog (Figure 4.2). Only spectra between 1 Hz and 10 Hz are plotted, as these are the dominant frequencies at this distance and do not include the microseism band below 1 Hz. From these comparative plots the difference in dominant frequency of each event type can be seen. A simple ratio of the maximum value between 3Hz and 5Hz divided by the maximum value between 6.5Hz and 8Hz was chosen to combine the most divergent frequency bands of the two different source types into a single value. For all magnitudes, the ratio for tectonic events is close to one, but the ratio for MIS, the ratio is much larger than one due to the lack of energy in the 6.5 Hz to 8 Hz band.

Figure 4.3 shows the ratio of each ground truth event plotted against magnitude. It can be seen in this plot that there is considerable overlap in the spectral ratio between the two event types. Importantly, however, there is a distinct range in the spectral ratio that only is seen in MIS. This pattern is constant across all magnitudes. Only two tectonic earthquakes plot with ratios greater than five, and these events, although outside the permit boundaries, are quite shallow. Using the spectral content of the seismogram is not as definitive as I had hoped, but it does provide an additional piece of information when considered together with the location, depth, first motions, and clustering information.

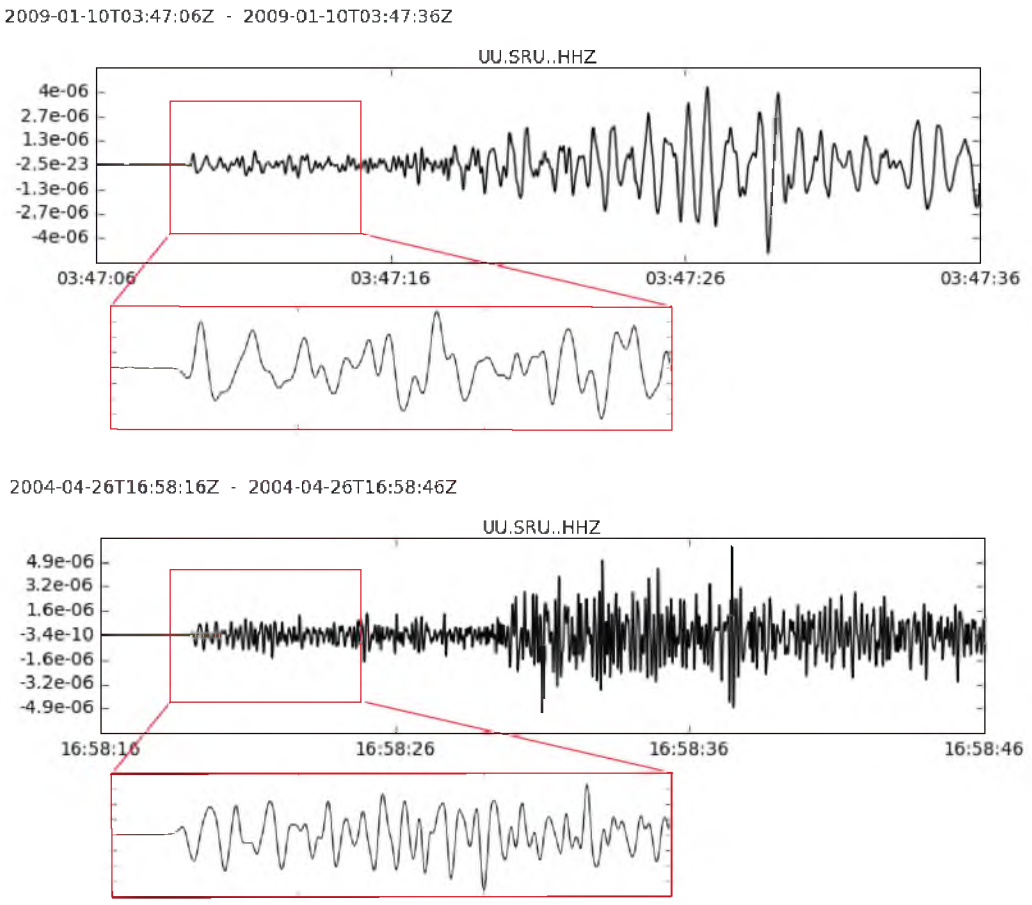

Figure 4.1. Difference in known source types. The top figure is a known mining event and the bottom is a known earthquake. Both waveforms are from the vertical component of SRU filtered between 1 Hz and 10 Hz cut to 30 sec starting 3 sec before the P-pick time. Both events have magnitude of 2.4 ($M_{L,}$) and the distance to station SRU is ~85 km and ~75 km, respectively. Expanded sections show initial 5 sec of energy.

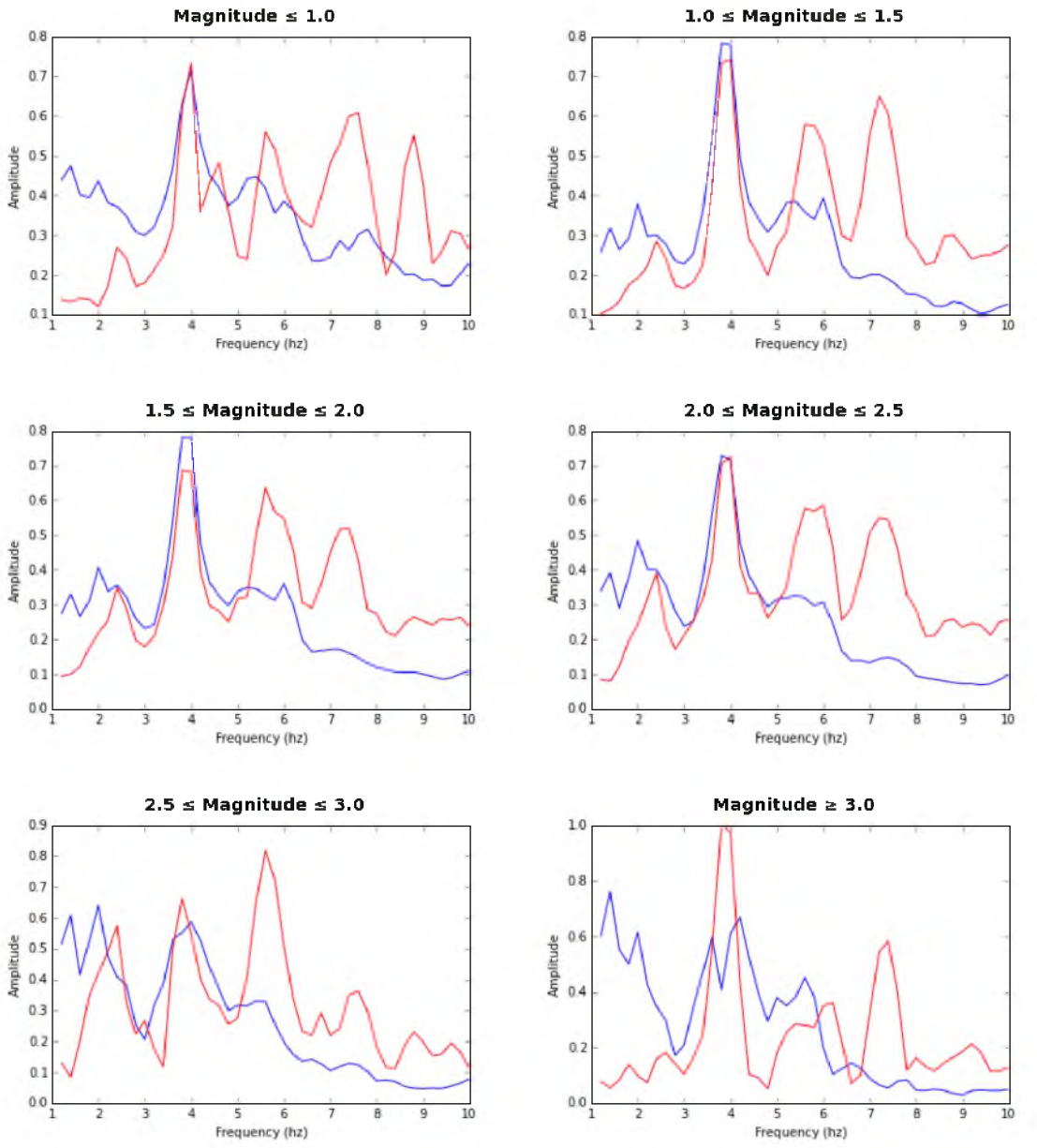

Figure 4.2. Average spectral plots. Spectral energy binned by magnitude for clusters and isolated events of known source type for MIS (blue) and tectonic earthquakes (red). Spectral ratio was determined from the difference in normalized amplitude between the 3 Hz to 5 Hz band and the 6.5 Hz to 8 Hz band.

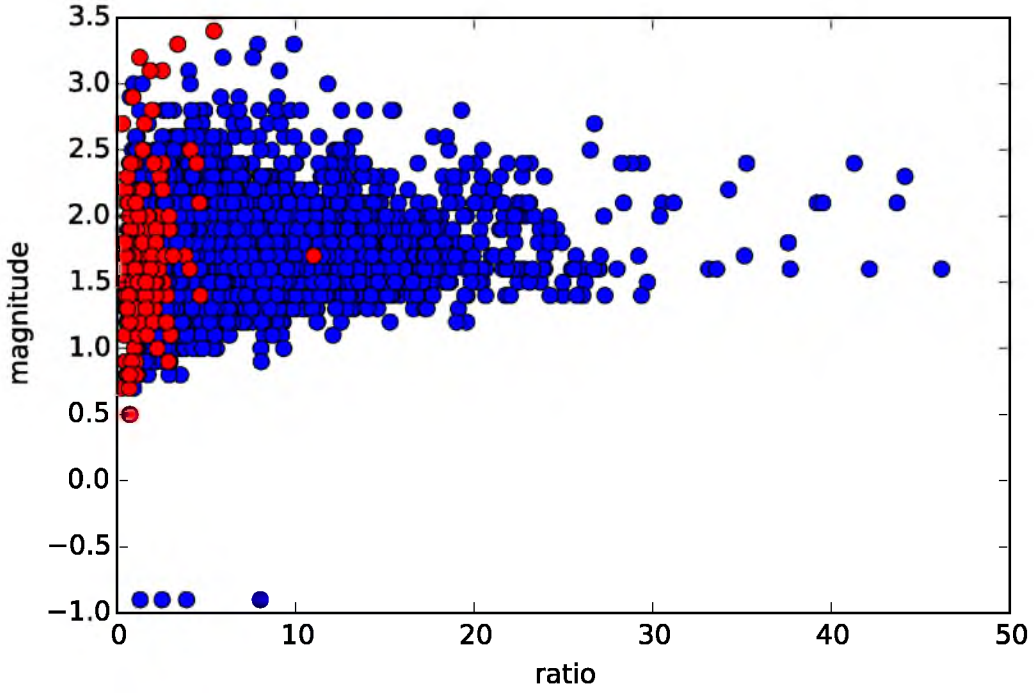

Figure 4.3. Known spectral ratios by magnitude. Each dot is a seismic event known to be either MIS (blue) or from a tectonic earthquake (red). The X-axis is the ratio of the maximum amplitude in the 3Hz to 5Hz band divided by the maximum amplitude in the 6.5 Hz to 8 Hz band. The Y-axis represents the Mc magnitude of each event.

CHAPTER 5

RESULTS AND DISCUSSION

Through the course of this study, I have examined the earthquake catalog of the Wasatch Plateau: updated event locations, performed waveform cross-correlation, examined first motions, and calculated spectral content. None of these methods on its own could sufficiently discriminate the source type of each event, but using all of the methods together provides much more evidence.

5.1 Combining the Various Discrimination Methods

To combine the different analyses for use in discrimination, I assigned a score to each cluster (Figure 5.1). Clusters were given a number of points based on the certainty of each method's ability to discriminate the source type, as determined during the analysis of each potential discriminant. For example, if events are outside of the mine permit boundaries or the cluster contains more than 50 events, the cluster was immediately classified as an earthquake cluster or MIS cluster, respectively. Only 5 points were added to either category if more or less than 50% of the events in a cluster had mixed first motions because first motions contribute little to discrimination of event type. A score of 100 points was required to categorize a cluster as MIS or earthquakes. If

this score was not reached, the cluster was classified as "Other."

Following the procedure in Figure 5.1, first, clusters located well outside of mine permit boundaries were classified as earthquakes. Although depth precision in the region is relatively low, the horizontal error is typically less than a kilometer, so events taking place ~3 km or more outside of permit boundaries could safely be categorized as earthquakes without further analysis. Next, clusters that contain more than 50 events were determined to be MIS, as it is known from previous studies [*Arabasz and Pechmann*, 2001] that most of the events in this region are MIS, and this is a larger number of events than in a typical earthquake swarm. Next, the spectral plots were analyzed. Clusters were considered to be more likely to be MIS if half or more of the events had spectral ratios of 3-5 Hz to 6.5-8 Hz energy greater than 5, and 95 points were added to the MIS score. Alternatively, if 90% or more of the ratio values were less than 3, it was considered to likely be an earthquake cluster, and 75 points were added to the earthquake score. Next, if the median depth of the cluster was above sea level, the cluster was considered likely to be MIS, and if median depth of the cluster was equal to or deeper than 5 km, it was considered that it was likely made up of earthquakes. Due to the uncertainty in resolving depth, only 50 points were added for either of these conditions. The first motions were the final and smallest addition. If a cluster was made up of events with less than half of the events as mixed first motions, then the cluster was slightly more likely to be MIS, and if more than half were mixed, it was slightly more likely to be a cluster of earthquakes contributing just 5 points for either case. Finally, the cluster was classified either as MIS or tectonic earthquake events if the cumulative MIS or earthquake score summed to 100 points or more. If a score of 100 was not reached for either total, the cluster was left as

unknown. The scores for each cluster can be found in the Appendix included with this document.

For example, Figure 5.2 shows examples for an MIS and earthquake cluster. The size of Cluster 0 and the location of Cluster 14 score 100 points for MIS and earthquake, respectively, and therefore further scoring is unnecessary. However, to illustrate the rest of the scoring, most spectral ratios in Cluster 0 are >5 (95 points), and 7.04% of the events have mixed first motions (5 points), yielding a total MIS score of 200 points. All spectral ratios in Cluster 14 are < 3 (75 points), and the median depth is 11.37 km (50 points), yielding a total EQ score of 225 points. In contrast, Figure 5.3 shows an example for a cluster that could not be discriminated, Cluster 34. Although it is located within the southernmost mine permit boundary and only has one event with a mixed first motion (suggesting that it is MIS), it has a wide range of spectral ratio values and a median depth of 3.6 km. As a result of these inconsistencies, this cluster was not assigned a source type (total MIS points 5; total EQ points 0).

A waveform comparison between an event from unclassified Cluster 22 and a nearby event classified as an earthquake from Cluster 44 (Figure 5.4) shows why the source type of some clusters remains unknown. Although the waveform from Cluster 22 has an impulsive first motion like that of the earthquake, it also contains significantly more long period energy throughout the event which is more typical of MIS. This particular cluster is located within a mine permit boundary, but there are earthquake clusters nearby, making confident discrimination inconclusive.

Events determined to be MIS events are shown in Figure 5.5 and can been seen to make up the vast majority (81.6%) of seismicity in the study area. Figure 5.6 shows the

865 events (13.5%) that could not be categorized and the 310 events (4.9%) determined to be tectonic in origin. Table 5.1 summarizes the results of the discrimination process. An electronic supplement contains a more detailed catalog of the 6,402 events analyzed in this study and can be downloaded at http://www.quake.utah.edu/EQCENTER/LISTINGS/utahregion.htm as a comma separated values file.

5.2 Influence of Injection Wells

During the course of this study, it was discovered that there are wastewater injection wells at the eastern edge of the study area (Figure 5.2) that have a small number of closely located events. Since these wells are outside of the mine permit boundaries, any event that occurred near a well was automatically classified as a tectonic earthquake even though their source may be related to the presence of the injection wells. This study does not attempt to definitively determine whether events near these injection wells are induced by fluid pressure or coincidental tectonic events, but 25 of the 310 tectonic events have been marked separately to indicate uncertainty in this area. No conclusion has been made about their source other than to say that they are not MIS. These events are represented as red triangles in Figure 5.6.

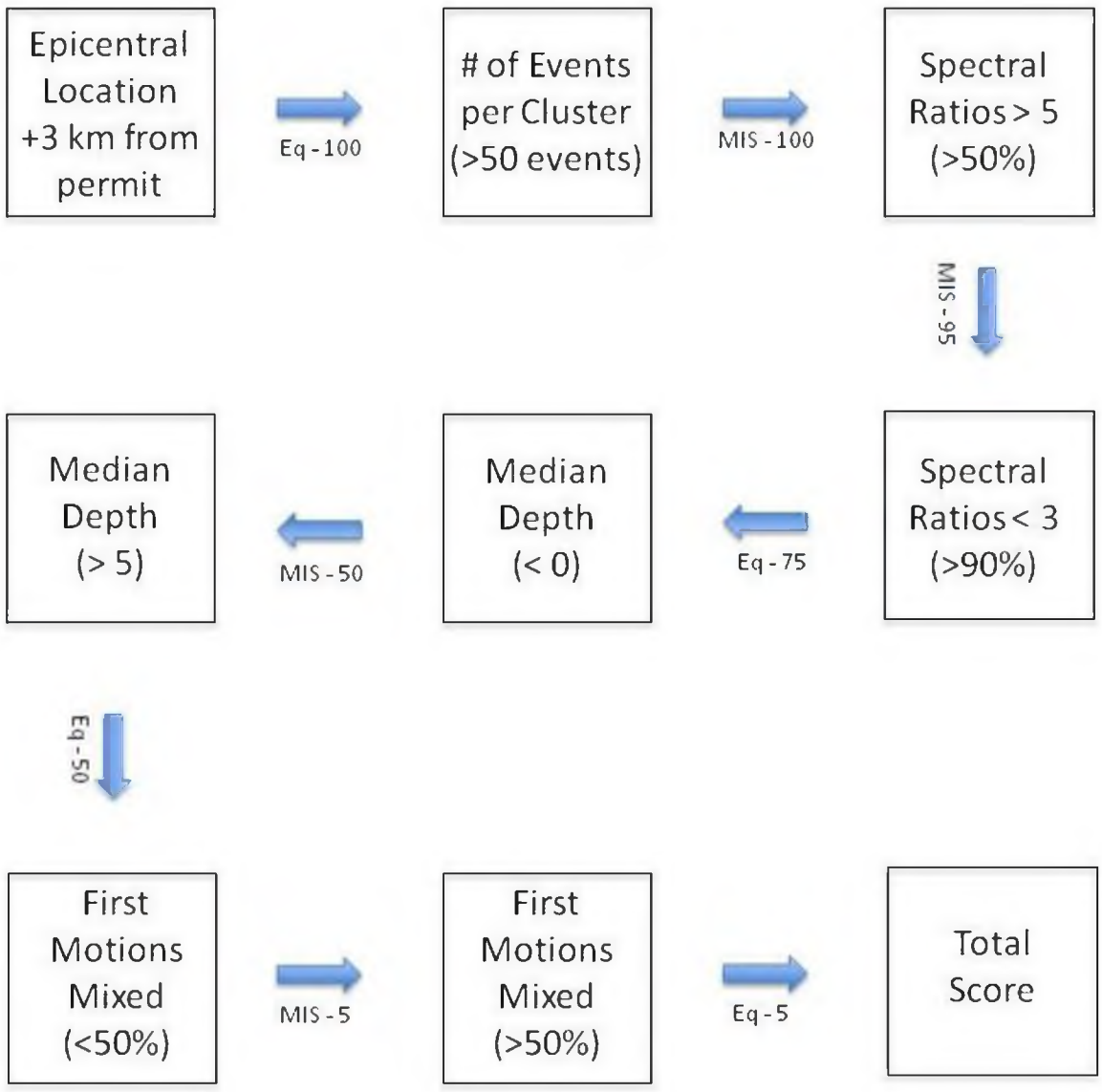

Figure 5.1. Cluster scoring. Discriminant categories are in boxes. Weights listed with arrows are assigned to each of the methods. A score of 100 is necessary to determine if a cluster is made up of MIS or earthquakes.

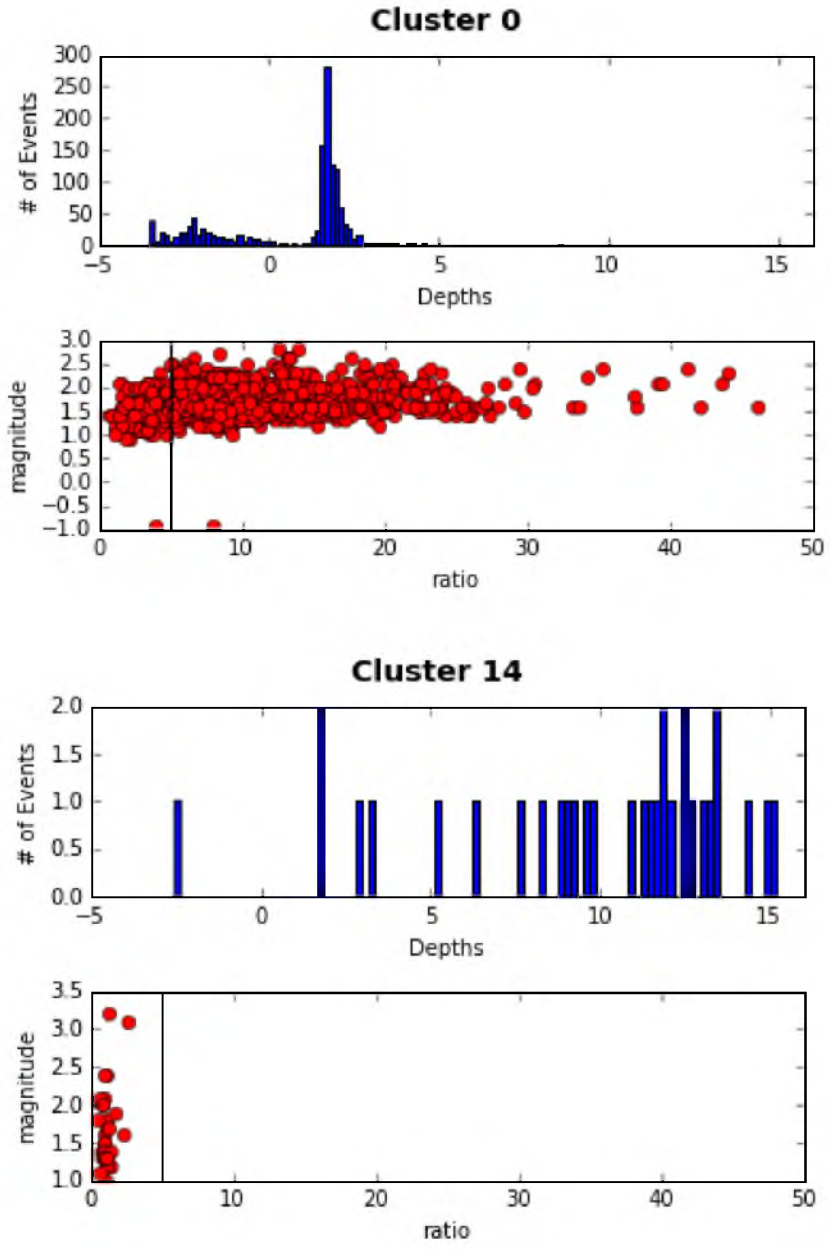

Figure 5.2. Depth and ratio plots. Cluster 0 is a known MIS cluster located within a mine permit boundary, where most events are shallow (less than 2 km), and the ratio values plot predominantly above 5.0. Cluster 14 is a known earthquake cluster located well outside of the mining region, depths vary but average 7.33 km, and all of ratio values plot well below 5.0.

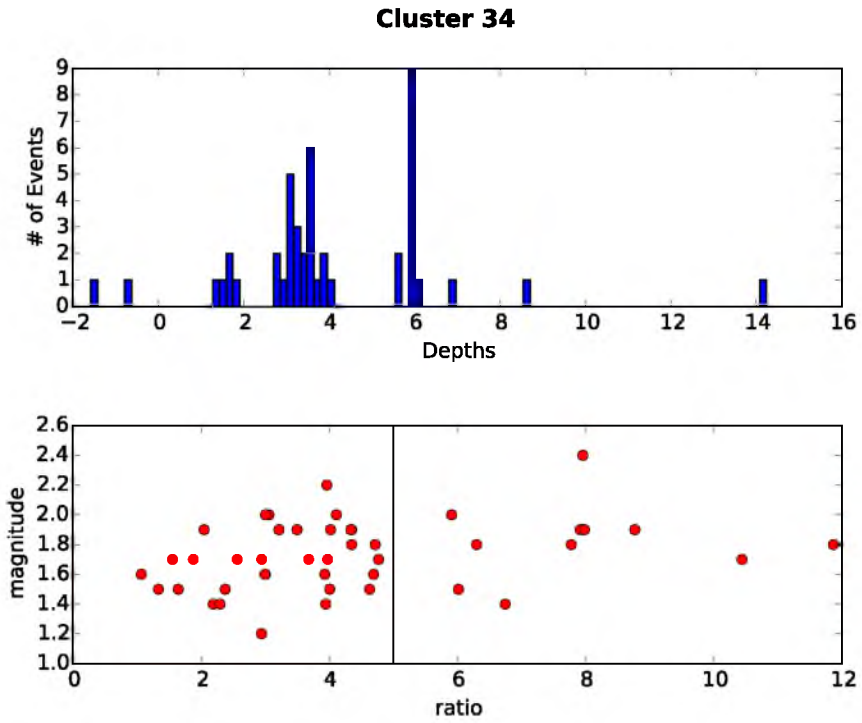

Figure 5.3. Individual cluster analysis. The source type of Cluster 34 could not be determined due to insufficient size (45 events), location within a permit boundary, the wide spread in event depths (top) and spectral ratios (bottom), and only one event (2.22%) with a mixed first motion in the event list.

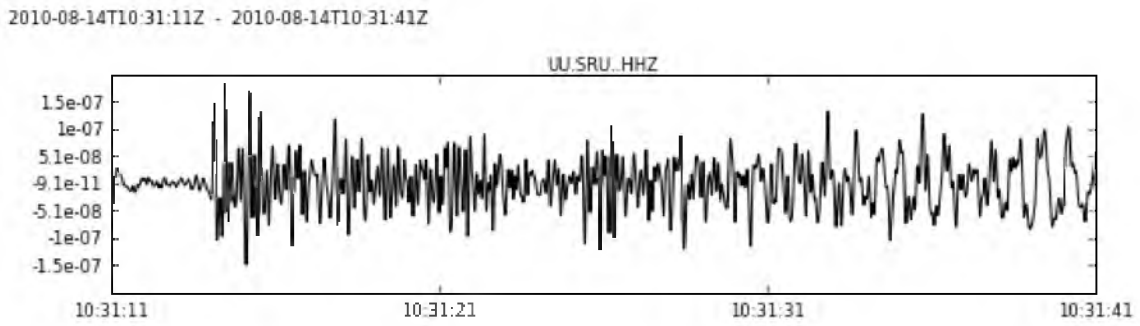

Cluster 22 Other

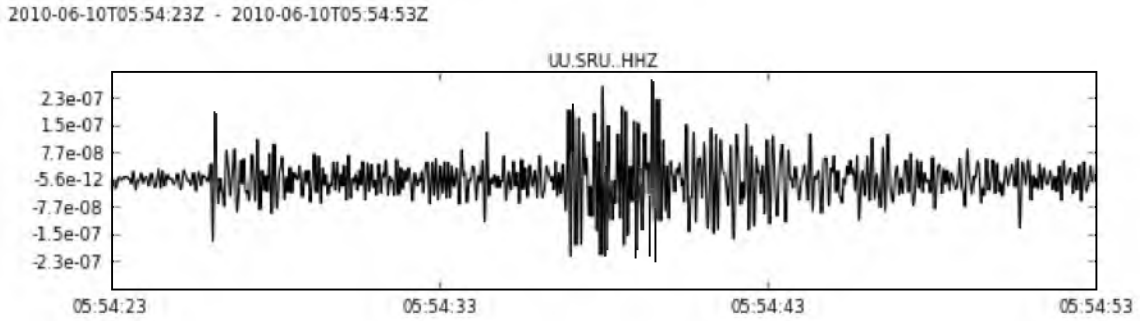

Cluster 44 Earthquake

Figure 5.4. Waveform comparison of other to earthquake. The top event belongs to the Cluster 22 of undetermined source type while bottom waveform is one of three in Cluster 44 determined to be earthquakes for comparison. The top waveform shows a combination of discrimination features with an impulsive first motion characteristic of earthquakes, but long period energy more similar to the MIS events.

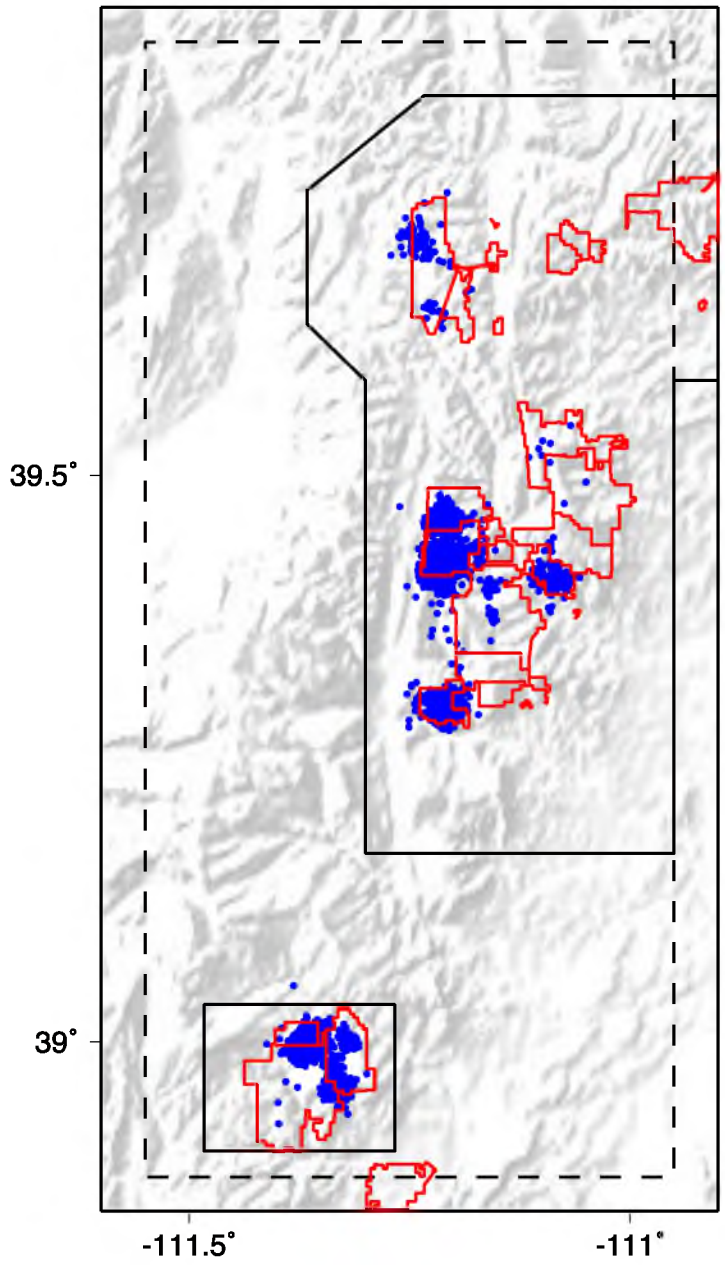

Figure 5.5. MIS events. Map of 5,227 events (blue dots) classified as MIS. Dashed box contains the region of focus for this study. Individual mine permit boundaries are illustrated with red polygons, the boundary of the mining region is shown as thin black polygons.

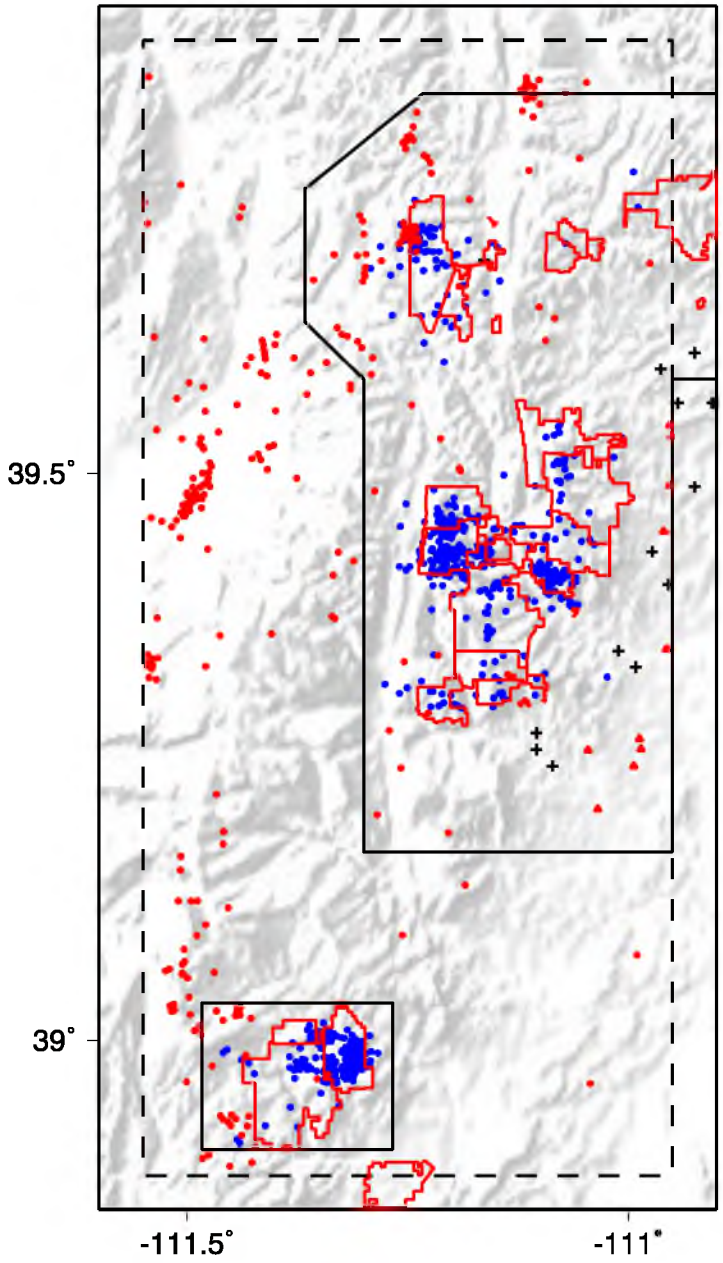

Figure 5.6. Non-MIS events. Map of 865 unclassified events (blue dots), 285 events classified as tectonic earthquakes (red dots), and 25 earthquake events determined to be influenced by nearby injection wells (red triangles). Black crosses are locations of fluid injection wells. The dashed box contains the region of focus for this study, individual mine permit boundaries are red polygons, and the boundary of the mining region is shown as thin black polygons.

Table 5.1 Results of aggregate discrimination methods

Event Type	Total Events	Clustered Events	Isolated Events	Number of Clusters
MIS	5227	5227	0	38
Earthquakes	285	186	99	42
Well Area	25	15	10	4
Other	865	704	161	81
Totals	6402	6132	270	165

CHAPTER 6

CONCLUSION

After applying several different discrimination methods to an earthquake catalog containing unknown seismic source types, I was able to discriminate ~86.5 % of the events as either MIS or tectonic earthquakes, leaving ~13.5% of the events unclassified. There are some events categorized as earthquakes within the mine permit boundaries in the northern, central, and southern permit boundaries. The unclassified events within mine permit boundaries are likely a mixture of both MIS and tectonic earthquakes. The northern portion of the study area appears to contain a zone of seismicity stretching southwest to northeast across the northernmost mine permit boundary.

Given the number of earthquakes found in this study (~5%) and the number of unclassified events, I conclude that less than 10% of the events in this study region are tectonic. This is important in regard to seismic hazard analysis of the region, because it implies that, despite the relatively large number of overall seismic events taking place in this region, very few reflect the release of tectonic strain. MIS is the result of removing material from a localized area, so any event listed as MIS can be largely ignored when determining seismic hazard.

The method used in this study of source discrimination based on multiple factors

leaves a notable population of events of unknown source, but this is partly due to the high level of agreement required in order to confidently classify a cluster. Depth resolution still remains to be a problem as location programs struggle to account for the shallow nature of MIS. Additional confidence could be added to the spectral analysis by more closely examining the signal to noise ratio of each event and additional attention could be given to peak frequencies at differing magnitudes. Additionally, more recent events have the benefit of more seismic stations resulting in somewhat better constraints on event location and a higher likelihood of accurate first motions. Ultimately, the vast majority of events have been categorized by source type in a catalog providing greater insight for future studies in this region.

APPENDIX

TABLE OF CLUSTER SCORES

Clust #	Type	Location to Permits	Events in Cluster	Spectral Ratios % > 5	Spectral Ratios % < 3	Median Depth	First Motions % Mixed	Score MIS	Score Eq
0	**MIS**	In	1341	82.85%	4.70%	1.65	7.04%	**200**	**0**
1	**MIS**	In	356	28.93%	40.45%	1.78	3.93%	**105**	**0**
2	**MIS**	In	61	27.87%	40.98%	-0.97	3.28%	**155**	**0**
3	**MIS**	In	105	18.10%	53.33%	1.70	3.81%	**105**	**0**
4	**Other**	In	3	33.33%	0.00%	4.63	0.00%	**5**	**0**
5	**MIS**	In	113	7.96%	76.11%	1.66	1.77%	**105**	**0**
6	**MIS**	In	34	67.65%	2.94%	3.21	20.59%	**100**	**0**
7	**MIS**	In	236	20.34%	32.20%	2.97	2.12%	**105**	**0**
8	**Other**	In	3	0.00%	33.33%	1.62	0.00%	**5**	**0**
9	**Other**	In	13	7.69%	84.62%	3.35	0.00%	**5**	**0**
10	**MIS**	In	177	3.95%	71.75%	3.20	26.55%	**105**	**0**
11	**Other**	In	18	22.22%	22.22%	1.83	5.56%	**5**	**0**
12	**MIS**	In	155	16.13%	50.32%	1.66	3.87%	**105**	**0**
13	**Eq**	Out	8	0.00%	100.00%	6.25	62.50%	**0**	**230**
14	**Eq**	Out	32	0.00%	100.00%	11.37	34.38%	**5**	**225**
15	**MIS**	In	110	10.91%	62.73%	1.63	1.82%	**105**	**0**
16	**MIS**	In	94	23.40%	40.43%	2.59	3.19%	**105**	**0**
17	**MIS**	In	180	10.00%	66.11%	1.68	1.11%	**105**	**0**
18	**MIS**	In	2	100.00%	0.00%	2.32	0.00%	**100**	**0**
19	**MIS**	In	182	33.52%	29.12%	5.50	0.55%	**105**	**50**
20	**MIS**	In	870	76.32%	7.70%	3.07	1.49%	**200**	**0**
21	**MIS**	In	65	6.15%	84.62%	-1.34	12.31%	**155**	**0**
22	**Other**	In	14	21.43%	35.71%	-1.28	14.29%	**55**	**0**
23	**Eq**	In	3	0.00%	100.00%	6.88	33.33%	**5**	**125**
24	**Eq**	Out	2	0.00%	100.00%	2.37	0.00%	**5**	**175**
25	**Eq**	Out	3	0.00%	100.00%	5.74	100.00%	**0**	**230**
26	**Other**	In	3	0.00%	100.00%	1.73	0.00%	**5**	**75**
27	**Other**	In	25	16.00%	12.00%	5.97	12.00%	**5**	**50**
28	**Other**	In	29	48.28%	10.34%	3.34	0.00%	**5**	**0**
29	**MIS**	In	4	50.00%	25.00%	-0.34	0.00%	**150**	**0**
30	**MIS**	In	3	100.00%	0.00%	1.44	0.00%	**100**	**0**
31	**Eq**	In	2	0.00%	100.00%	11.35	0.00%	**5**	**125**
32	**Eq**	Out	2	0.00%	100.00%	5.50	50.00%	**0**	**230**
33	**Other**	In	2	0.00%	50.00%	1.67	50.00%	**0**	**5**
34	**Other**	In	45	26.67%	28.89%	3.60	2.22%	**5**	**0**
35	**Eq**	Out	3	0.00%	33.33%	5.29	100.00%	**0**	**155**
36	**MIS**	In	110	10.00%	45.45%	2.94	1.82%	**105**	**0**
37	**MIS**	In	295	1.69%	89.83%	1.61	0.34%	**105**	**0**
38	**Other**	In	5	20.00%	20.00%	3.04	0.00%	**5**	**0**
39	**Other**	In	31	0.00%	54.84%	1.84	3.23%	**5**	**0**
40	**Other**	In	10	0.00%	100.00%	3.85	0.00%	**5**	**75**

Clust #	Type	Location to Permits	Events in Cluster	Spectral Ratios % > 5	Spectral Ratios % < 3	Median Depth	First Motions % Mixed	Score MIS	Score Eq
41	**Eq**	Out	2	0.00%	100.00%	14.11	100.00%	**0**	**230**
42	**Other**	In	9	11.11%	33.33%	3.57	0.00%	**5**	**0**
43	**Other**	In	2	0.00%	100.00%	1.41	0.00%	**5**	**75**
44	**Eq**	Out	3	0.00%	100.00%	11.47	33.33%	**5**	**225**
45	**Other**	In	2	0.00%	100.00%	3.19	50.00%	**0**	**80**
46	**Other**	In	2	0.00%	50.00%	1.86	50.00%	**0**	**5**
47	**MIS**	In	2	50.00%	0.00%	1.64	0.00%	**100**	**0**
48	**Other**	In	16	18.75%	31.25%	2.32	0.00%	**5**	**0**
49	**Other**	In	2	0.00%	100.00%	1.62	0.00%	**5**	**75**
50	**MIS**	In	204	2.94%	71.57%	3.38	13.24%	**105**	**0**
51	**Other**	In	41	41.46%	21.95%	7.14	0.00%	**5**	**50**
52	**MIS**	In	76	6.58%	61.84%	3.58	15.79%	**105**	**0**
53	**Other**	In	32	15.63%	18.75%	2.88	0.00%	**5**	**0**
54	**MIS**	In	68	19.12%	36.76%	5.87	0.00%	**105**	**50**
55	**Eq**	Out	3	0.00%	100.00%	5.58	100.00%	**0**	**230**
56	**MIS**	In	82	9.76%	75.61%	1.54	0.00%	**105**	**0**
57	**Eq**	Out	6	0.00%	100.00%	7.66	16.67%	**5**	**225**
58	**Other**	In	4	0.00%	100.00%	2.06	50.00%	**0**	**80**
59	**Other**	In	15	0.00%	100.00%	1.70	6.67%	**5**	**75**
60	**Eq**	Out	8	0.00%	100.00%	2.41	62.50%	**0**	**180**
61	**Other**	In	24	12.50%	83.33%	1.91	0.00%	**5**	**0**
62	**MIS**	In	83	50.60%	4.82%	1.02	10.84%	**200**	**0**
63	**Other**	In	18	0.00%	94.44%	1.80	0.00%	**5**	**75**
64	**Other**	In	7	42.86%	14.29%	0.16	0.00%	**5**	**0**
65	**MIS**	In	88	10.23%	54.55%	3.29	10.23%	**105**	**0**
66	**Eq**	In	23	0.00%	95.65%	5.98	4.35%	**5**	**125**
67	**Eq**	Out	2	0.00%	100.00%	2.57	0.00%	**5**	**175**
68	**Other**	In	7	0.00%	100.00%	1.74	0.00%	**5**	**75**
69	**Other**	In	27	3.70%	88.89%	2.68	0.00%	**5**	**0**
70	**Eq**	Out	8	0.00%	100.00%	13.14	100.00%	**0**	**230**
71	**MIS**	In	2	50.00%	0.00%	-1.91	0.00%	**150**	**0**
72	**Other**	In	3	0.00%	100.00%	-0.14	0.00%	**55**	**75**
73	**Other**	In	4	0.00%	100.00%	1.88	0.00%	**5**	**75**
74	**Other**	In	13	30.77%	23.08%	3.37	0.00%	**5**	**0**
75	**MIS**	In	2	100.00%	0.00%	4.64	0.00%	**100**	**0**
76	**Eq**	Out	2	0.00%	100.00%	-2.22	0.00%	**55**	**175**
77	**Other**	In	2	0.00%	0.00%	2.25	0.00%	**5**	**0**
78	**Other**	In	10	10.00%	80.00%	2.11	10.00%	**5**	**0**
79	**Eq**	Out	3	0.00%	100.00%	14.48	66.67%	**0**	**230**
80	**Other**	In	7	0.00%	100.00%	1.88	0.00%	**5**	**75**

Clust #	Type	Location to Permits	Events in Cluster	Spectral Ratios % > 5	Spectral Ratios % < 3	Median Depth	First Motions % Mixed	Score MIS	Score Eq
81	**Eq**	Out	2	0.00%	50.00%	3.17	0.00%	**5**	**100**
82	**Other**	In	3	0.00%	66.67%	-2.32	0.00%	**55**	**0**
83	**Eq**	Out	12	0.00%	100.00%	4.53	50.00%	**0**	**180**
84	**Other**	In	19	15.79%	31.58%	2.85	10.53%	**5**	**0**
85	**Other**	In	3	0.00%	100.00%	3.20	0.00%	**5**	**75**
86	**Other**	In	21	14.29%	33.33%	3.28	4.76%	**5**	**0**
87	**Other**	In	2	0.00%	50.00%	3.72	0.00%	**5**	**0**
88	**Other**	In	4	0.00%	100.00%	2.70	0.00%	**5**	**75**
89	**Other**	In	3	0.00%	66.67%	0.84	0.00%	**5**	**0**
90	**Eq**	Out	6	0.00%	100.00%	4.76	50.00%	**0**	**180**
91	**Other**	In	4	0.00%	25.00%	1.80	0.00%	**5**	**0**
92	**Other**	In	8	0.00%	100.00%	2.91	12.50%	**5**	**75**
93	**MIS**	In	54	38.89%	16.67%	3.90	11.11%	**105**	**0**
94	**MIS**	In	3	100.00%	0.00%	2.95	0.00%	**100**	**0**
95	**Other**	In	10	0.00%	90.00%	1.70	0.00%	**5**	**75**
96	**Other**	In	15	0.00%	80.00%	3.60	0.00%	**5**	**0**
97	**Eq**	In	3	0.00%	100.00%	5.94	66.67%	**0**	**130**
98	**Other**	In	3	33.33%	66.67%	-2.05	0.00%	**55**	**0**
99	**Eq**	Out	2	0.00%	100.00%	8.12	0.00%	**5**	**225**
100	**Other**	In	3	33.33%	66.67%	2.33	33.33%	**5**	**0**
101	**Other**	In	2	0.00%	100.00%	1.71	0.00%	**5**	**75**
102	**Other**	In	2	0.00%	100.00%	2.12	0.00%	**5**	**75**
103	**Other**	In	2	0.00%	100.00%	1.47	0.00%	**5**	**75**
104	**Other**	In	2	0.00%	0.00%	1.66	0.00%	**5**	**0**
105	**Other**	In	5	0.00%	80.00%	1.62	0.00%	**5**	**0**
106	**Other**	In	2	0.00%	50.00%	1.66	0.00%	**5**	**0**
107	**MIS**	In	11	90.91%	0.00%	1.59	0.00%	**100**	**0**
108	**Other**	In	2	0.00%	100.00%	4.92	50.00%	**0**	**80**
109	**Other**	In	8	12.50%	62.50%	3.30	0.00%	**5**	**0**
110	**Other**	In	2	0.00%	50.00%	1.63	0.00%	**5**	**0**
111	**Other**	In	4	0.00%	75.00%	1.71	0.00%	**5**	**0**
112	**Eq**	Out	4	0.00%	100.00%	8.99	0.00%	**5**	**225**
113	**Other**	In	14	7.14%	71.43%	2.67	0.00%	**5**	**0**
114	**Other**	In	8	0.00%	62.50%	-0.70	0.00%	**55**	**0**
115	**Other**	In	9	0.00%	77.78%	3.72	22.22%	**5**	**0**
116	**Other**	In	5	0.00%	40.00%	1.84	0.00%	**5**	**0**
117	**Other**	In	27	0.00%	100.00%	1.69	0.00%	**5**	**75**
118	**MIS**	In	3	66.67%	0.00%	3.30	0.00%	**100**	**0**
119	**MIS**	In	3	66.67%	33.33%	0.97	0.00%	**100**	**0**
120	**Other**	In	5	40.00%	0.00%	2.97	40.00%	**5**	**0**

Clust #	Type	Location to Permits	Events in Cluster	Spectral Ratios % > 5	Spectral Ratios % < 3	Median Depth	First Motions % Mixed	Score MIS	Score Eq
121	**Eq**	Out	3	0.00%	100.00%	2.94	66.67%	**0**	**180**
122	**Other**	In	7	0.00%	100.00%	1.67	0.00%	**5**	**75**
123	**MIS**	In	16	56.25%	0.00%	5.97	0.00%	**100**	**50**
124	**Eq**	Out	4	0.00%	100.00%	3.84	0.00%	**5**	**175**
125	**Other**	In	5	40.00%	20.00%	-1.59	20.00%	**55**	**0**
126	**Other**	In	6	16.67%	16.67%	0.93	0.00%	**5**	**0**
127	**Eq**	Out	2	0.00%	100.00%	1.90	100.00%	**0**	**180**
128	**Eq**	Out	2	0.00%	100.00%	12.93	0.00%	**5**	**225**
129	**Other**	In	4	0.00%	75.00%	-2.84	25.00%	**55**	**0**
130	**Eq**	Out	2	0.00%	100.00%	9.45	0.00%	**5**	**225**
131	**Other**	In	3	0.00%	33.33%	9.46	0.00%	**5**	**50**
132	**Eq**	Out	2	0.00%	100.00%	3.08	100.00%	**0**	**180**
133	**MIS**	In	21	66.67%	23.81%	-2.95	38.10%	**150**	**0**
134	**Other**	In	2	0.00%	100.00%	0.58	0.00%	**5**	**75**
135	**Other**	In	7	0.00%	71.43%	3.63	0.00%	**5**	**0**
136	**Eq**	Out	6	0.00%	100.00%	9.31	16.67%	**5**	**225**
137	**Eq**	Out	2	0.00%	100.00%	9.54	100.00%	**0**	**230**
138	**Other**	In	2	0.00%	100.00%	1.66	0.00%	**5**	**75**
139	**Other**	In	2	0.00%	100.00%	-2.82	50.00%	**50**	**80**
140	**Other**	In	4	25.00%	25.00%	1.52	0.00%	**5**	**0**
141	**Eq**	Out	6	0.00%	100.00%	9.14	66.67%	**0**	**230**
142	**Other**	In	3	0.00%	100.00%	2.09	100.00%	**0**	**80**
143	**Eq**	Out	3	0.00%	100.00%	5.94	33.33%	**5**	**225**
144	**Other**	In	2	0.00%	100.00%	2.15	0.00%	**5**	**75**
145	**Other**	In	2	0.00%	100.00%	0.80	50.00%	**0**	**80**
146	**MIS**	In	6	83.33%	0.00%	1.98	0.00%	**100**	**0**
147	**MIS**	In	3	100.00%	0.00%	-1.17	0.00%	**150**	**0**
148	**Eq**	Out	2	0.00%	100.00%	13.00	100.00%	**0**	**230**
149	**Eq**	Out	2	0.00%	100.00%	15.61	50.00%	**0**	**230**
150	**Other**	In	2	0.00%	0.00%	6.12	0.00%	**5**	**50**
151	**Other**	In	2	0.00%	100.00%	1.09	50.00%	**0**	**80**
152	**Other**	In	2	0.00%	0.00%	0.91	100.00%	**0**	**5**
153	**Eq**	Out	2	0.00%	100.00%	10.83	0.00%	**5**	**225**
154	**Eq**	Out	2	0.00%	100.00%	10.74	0.00%	**5**	**225**
155	**Eq**	In	2	0.00%	100.00%	14.76	0.00%	**5**	**125**
156	**Eq**	Out	2	0.00%	100.00%	2.22	0.00%	**5**	**175**
157	**Eq**	Out	2	100.00%	0.00%	5.55	100.00%	**95**	**155**
158	**Eq**	In	2	0.00%	100.00%	5.93	0.00%	**5**	**125**
159	**Eq**	In	2	0.00%	100.00%	5.12	0.00%	**5**	**125**
160	**Other**	In	2	0.00%	100.00%	-1.00	0.00%	**55**	**75**

Clust		Location	Events in	Spectral Ratios		Median	First Motions	Score	
#	**Type**	to Permits	Cluster	% > 5	% < 3	Depth	% Mixed	**MIS**	**Eq**
161	**Eq**	Out	2	0.00%	100.00%	20.58	100.00%	**0**	**230**
162	**Eq**	In	2	0.00%	100.00%	5.50	100.00%	**0**	**130**
163	**Other**	In	2	0.00%	0.00%	5.84	0.00%	**5**	**50**
164	**Eq**	Out	2	0.00%	100.00%	4.31	100.00%	**0**	**180**

REFERENCES

Allmann, B. P., P. M. Shearer, and E. Hauksson (2008), Spectral discrimination between quarry blasts and earthquakes in Southern California. *Bull. Seismol. Soc. Am.*, *98*(4), 2073-2079.

Arabasz, W. J., R. Burlacu, and K. Pankow (2007), An overview of historical and contemporary seismicity in central Utah. *Central Utah: Diverse Geology of a Dynamic Landscape*, *36*(4), 540.

Arabasz, W. J., and J. C. Pechmann (2001), Seismic characterization of coal-mining seismicity in Utah for CTBT monitoring. *Lawrence Livermore National Laboratory internal report UCRL-CR-143772*.

Arabasz, W. J., S. J. Nava, and W. T. Phelps (1997). Mining seismicity in the Wasatch Plateau and Book Cliffs coal mining districts, Utah, USA, In *Rockbursts and Seismicity in Mines*, S. J. Gibowicz and S. Lasocki (Editors), A. A. Balkema, Rotterdam, 111-116

Arrowsmith, S. J., and L. Eisner (2006), A technique for identifying microseismic multiplets and application to the Valhall field, North Sea. *Geophys. 71*(2), 31-40.

Baisch, S., L. Ceranna, and H. P. Harjes (2008), Earthquake cluster: what can we learn from waveform similarity? *Bull. Seismol. Soc. Am.*, *98*(6), 2806-2814.

Boltz, M. S., K. L. Pankow, and M. K. McCarter (2014), Fine details of mining-induced seismicity at the Trail Mountain Coal Mine using modified hypocentral relocation techniques, *Bull. Seismol. Soc. Am.*, *104*(1), 193-203.

Beyreuther, M., R. Barsch, L. Krischer, T. Megies, Y. Behr, and J. Wassermann (2010), ObsPy: A Python toolbox for seismology. *Seismol. Res. Lett.*, *81*(3), 530-533.

Burlacu, R., P. M. Roberson, J. M. Hale, Y. H. Wong, and N. S. Mohammad Jamaal (2013), Earthquake activity in the Utah region: Preliminary epicenters October 1–December 31, 2012, *Quarterly Report of University of Utah Seismograph Stations*, [Available at http://www.seis.utah.edu/EQCENTER/QUARTERLY/ /REPORTS/2012/2012Q4.pdf.]

Chambers, D. J. A., K. D. Koper, K. L. Pankow, and M. K. McCarter (2015), Detecting and characterizing coal mine related seismicity in the Western U.S. using subspace methods, *Geophys. J. Inter.*, *203*(2), 1388-1399.

Ford, S. R., D. S. Dreger, and W. R. Walter (2008), Source characterization of the 6 August 2007 Crandall Canyon Mine seismic event in central Utah, *Seismol. Res. Lett.*, *79*(5), 637-644.

Gale, W. J., K. A. Heasley, A. T. Iannacchione, P. L. Swanson, P. Hatherly, and A. King (2001), Rock damage characterisation from microseismic monitoring. In *DC Rocks 2001, The 38th US Symposium on Rock Mechanics (USRMS)*. American Rock Mechanics Association, Washington, D.C.

Harris, D. B. (2006), Subspace detectors: Theory. *Lawrence Livermore National Laboratory Technical Report UCRL-TR-222758*, Livermore, CA.

Iannacchione, A. T., G. S. Esterhuizen, T. S. Bajpayee, P. L. Swanson, and M. C. Chapman (2005), Characteristics of mining-induced seismicity associated with roof falls and roof caving events. In *Alaska Rocks 2005, The 40th US Symposium on Rock Mechanics (USRMS)*. American Rock Mechanics Association.

Klein, F. W. (1978), *Hypocenter Location Program HYPOINVERSE.* U.S. Geol. Surv. Open File Report 78-694, 113.

Klein, F. W. (2001), User's Guide to Hypoinverse-2000, a Fortran Program to Solve for Earthquake Locations and Magnitudes (4/2002 version 1.0). U.S. Geol. Surv. Open File Report: 02-171.

Kubacki, T., K. D. Koper, K. L. Pankow, and M. K. McCarter (2014), Changes in mining-induced seismicity before and after the 2007 Crandall Canyon Mine collapse, *J. Geophys. Res. Solid Earth*, *119*(6), 4876-4889.

Pechmann, J. C., W. J. Arabasz, K. L. Pankow, R. Burlacu, and M. K. McCarter (2008), Seismological report on the 6 August 2007 Crandall Canyon mine collapse in Utah, *Seismol. Res. Lett.*, *79*(5), 620-636.

Petersen, M.D., M.P. Moschetti, P.M. Powers, C.S. Mueller, K.M. Haller, A.D. Frankel, Zeng, Yuehua, Rezaeian, Sanaz, S.C. Harmsen, O.S. Boyd, Field, Ned, Chen, Rui, K.S. Rukstales, Luco, Nico, R.L. Wheeler, R.A. Williams, and A.H. Olsen (2014), Documentation for the 2014 update of the United States national seismic hazard maps: U.S. Geological Survey Open-File Report 2014–1091, 243.

Petersen, M.D., C.S. Mueller, M.P. Moschetti, S.M. Hoover, J.L. Rubinstein, A.L. Llenos, A.J. Michael, W.L. Ellsworth, A.F. McGarr, A.A. Holland, and J.G. Anderson, (2015), Incorporating induced seismicity in the 2014 United States

National Seismic Hazard Model—Results of 2014 workshop and sensitivity studies: U.S. Geological Survey Open-File Report 2015–1070, 69.

Schaff, D. P., and F. Waldhauser (2010), One magnitude unit reduction in detection threshold by cross correlation applied to Parkfield (California) and China seismicity. *Bull. Seismol. Soc. Am.*, *100*(6), 3224-3238.

Smith, R. B., and W. J. Arabasz (1991), Seismicity of the Intermountain Seismic Belt, *Neotect. N. Am.*, (1), 185–228.

Stein, J.R., K. L. Pankow, K. D. Koper, and M. K. McCarter (2015), Discriminating Mining Induced Seismicity From Natural Tectonic Earthquakes in the Wasatch Plateau Region of Central Utah. 34st Int. Conf. on Ground Control in Min., Morgantown, WV.

Stein, S., and M. Wysession (2003), An Introduction to Seismology, Earthquakes, and Earth Structure, Blackwell Publishing Ltd., Malden, MA.

Stump, B., R. Burlacu, C. Hayward, J. Bonner, K. Pankow, A. Fisher, and S. Nava (2007), Seismic and infrasound energy generation and propagation at local and *Monitoring Res. Review,* Denver, CO, 25– 27 Sept.

Wong, I. G. (1985), Mining-induced earthquakes in the Book Cliffs and eastern Wasatch Plateau, Utah, USA. *Int. J. Rock Mech. Min. Sci. 22*(4), 263-270.

Zhang, M., and L. Wen (2015), Seismological evidence for a low-yield nuclear test on 12 May 2010 in North Korea. *Seismol. Res. Lett.*, *86*(1), 138-145.